DETAILED EXPERIMENTAL INVESTIGATION OF AIR SPEED FIELD INDUCED BY CEILING FANS

Shuo LIU [a], Aleksandra LIPCZYNSKA [a,*], Stefano SCHIAVON [b], and Edward ARENS [b]

[a] Berkeley Education Alliance for Research in Singapore Limited, Singapore

[b] Center for the Built Environment, University of California, Berkeley, United States

Abstract

Comfort cooling by ceiling fans is cost-effective and energy-efficient compared to compressor-based cooling and fans are commonly used in tropical and subtropical countries. There are however limited data and design tools supporting the design of fan systems, especially for situations where there are multiple fans. In this paper, we investigate airflow profiles induced by a single fan and multiple fans using high spatial resolution air speed measurements (5,760 and 20,160 measuring points for the two cases respectively) in a climatic chamber. To authors' knowledge, this is the first time that interaction between multiple fans has been reported. We developed typical airflow patterns from the measurements and further validated them via smoke visualization. The single-fan results are consistent with previous studies of this configuration, providing additional refinements. For the multiple-fan case, both the difference of fan speed levels and the distance between the fans affect the interacting airflow profiles of the fans in complex ways. When fans are close enough, the combined air speed profile cannot be extrapolated from the profile of a single fan. All the measurement results are open sourced: raw data is included in the supplementary materials and can be visualized via an online platform (single fan, multiple fans). The data and the tool can be used to validate CFD models and inform fan layout design.

Keywords: Ceiling fans, Air speed distribution, Fans interaction

Highlights

- Measured at high resolution the air speeds induced by a ceiling fan, and the interactions between multiple fans
- Developed generalized room airflow patterns for single and multiple fans
- Developed an Air Speed Range Coverage index to describe air speed distributions caused by ceiling fans
- Developed an online visualization tool of air speeds based on the measurement data

* Corresponding author:
Berkeley Education Alliance for Research in Singapore Limited, 1 CREATE Way #11-02, CREATE Tower, Singapore 138602, Singapore
e-mail address: aleksandra.lipczynska@bears-berkeley.sg

DOI: 10.1016/j.buildenv.2018.06.037
https://escholarship.org/uc/item/2mk3n264

1 Introduction

Raising the cooling set-point of compressor-based air conditioning systems saves substantial energy in humid and hot climates [1–5]. Electric fans can be used in conjunction to offset the impact of warmer temperatures on thermal comfort [6–11]. Ceiling fans are cost-effective and energy-efficient comfort cooling approaches commonly used in tropical and subtropical countries, mainly in residential buildings and semi-outdoor spaces. Compared to compressor-based cooling, ceiling fans cool people with less energy consumption [12] by enhancing convective heat transfer [13], and by creating more uniform air temperature distribution through increased air circulation [14,15]. Previous laboratory and field studies on human subjects have shown that using ceiling fans improves perceived air quality, sensation of thermal comfort and productivity [7,10,16–19]. Although being widely used in the residential sector [20], ceiling fans have rarely been incorporated into commercial buildings even though field study shows such need [16,20–24]. The hesitation to use fans in commercial spaces is probably due to lack of engineering-grade design information, the inherently non-uniform nature of the airflow, and thermal comfort standards that were unfavorable to the use of air movement for cooling. The international thermal comfort standards have in recent years included provisions for individual and group comfort under elevated air movement [25,26], but there were no metrics for quantifying comfort conditions when the air speeds are non-uniformly distributed, nor were there any design tools providing an approach to spacing and controlling fans within office rooms. Moreover, the changes in [25,26] might not be incorporated into national level regulations (e.g. [27]).

There have been quite a few tests of the patterns of air speed around single ceiling fans in empty rooms [12,28–30], but not many data sets are useful for detailed examination or development into design tools. Most of these measurements were performed in a single line of different radial distances starting from the fan center [29,31–34], assuming symmetry of the boundary conditions and fan jet distribution. Moreover, all of these studies were characterizing the flow from a single ceiling fan operating in an empty room. The same simplification is used in the draft of a new ASHRAE Standard on the quantifying the performance of ceiling fans [35]. The airflow induced by a ceiling fan may be simulated in varying levels of complexity with CFD models, and the techniques involved are still topics of research [31–33,36]. High flexibility in the use of possible tools for building computational models requires them to be validated with physical measurements. There has been a shortage of detailed experimental data for inputting boundary conditions [37] and for calibrating and validating models. The over-simplified models of a jet fan might be unreliable as they could create a false image of the jet shape, air speed values, coverage range and turbulence intensity. That is why physical measurements of air speed field provided with ceiling fans need to include more complex and realistic scenarios, i.e. impact of the room furnishing, location of heat sources, usage of multiple fans or impact of the ventilation system.

So far, Gao et al. [30] performed air speed measurements with a single ceiling fan, investigating the effects of desks and office partitions on the surrounding airflow, and quantifying the effects of the flow patterns on human comfort. They developed a simplified organizing model of room airflow for positioning fans relative to furnishings in design. The data are publicly available and have been used in a separate study to validate a computer model simulating the effects of fan blade shape, fan speed, and geometry of fan and ceiling [31]. More detailed measurement results like this, including for example placement of room heat sources or multiple fans are still missing. Relative performance of multiple fans has not been reported in the literature, while such information is crucial for successful

implementation of fans in large area spaces (e.g., open space offices). The designers need to receive tools addressing this concern to properly select fans' spacing and to optimize the fans' control [38].

In this paper, our objectives are to (1) provide very high spatial resolution air speed measurements over the whole occupied zone of a) one ceiling fan at various speeds and b) two ceiling fans at various speed levels and distances; (2) develop typical air speed profiles based on physical measurements and smoke visualization; (3) develop new indices to describe the space air speed uniformity and the fan interaction effects (see Appendix A); (4) develop an online database and interactive data visualization based on the measurement results of both single-fan and double-fan cases (see Appendix B).

2 Methodology

2.1 Experimental facilities

The experiments were conducted in two identical physical chambers (5.6 × 4.3 × 2.6 m) located at SinBerBEST in the CREATE Tower, Singapore. We did not include in this study the impact of furnishing, heat sources and ventilation flows on air distribution within the space.

Tests were done with Haiku H-Series ceiling fans with fan diameter of D = 1.5 m (60 in.; BigAss Solutions, US). They are equipped with an electronically commutated motor and a digital inverter drive, which provide seven speed levels. The power consumption and RPM (Revolutions Per Minute) corresponding to each fan speed level are described later. The power consumption and the RPM do not increase linearly with the speed level. The fan power was measured by a power meter (Energy monitoring socket, Efergy, UK) with an accuracy of ±2% of readings and the RPM was measured by a tachometer (Model 470, Testo, Germany) with a resolution of 0.1 rpm (+100 to +999.9 rpm) and an accuracy of ±0.02% of readings.

2.2 Fans configurations

All fans were mounted at the height of 2.3 m above the floor. The distance between fan blades and the ceiling was 0.3 m, allowing sufficient air circulation [31]. The mounting fixtures were stable, and fan blades were leveled and balanced to avoid wobbling. Fan blades rotated in a clockwise direction (top-to-bottom view), pushing air towards the floor.

As shown in Figure 1A, the ceiling fan in the single-fan room was installed in the central area of the chamber. The distances between the fan center and walls were at least 1.2 times the fan diameter (1.2xD). We measured air speeds for all fan speed levels (0 to 7). Before any measurements were taken, the fans were run for sufficient time to avoid initial transient phenomena.

In the double-fan room, we tested the interaction between two ceiling fans in three configurations with different center-to-center distances (1.3xD, 1.7xD and 2.1xD). Fans were installed in any two out of three positions, namely F1, F2 and F3 as shown in Figure 1B. We measured air speed with various combinations of speed levels for each fan (level 0 – turned off, level 1 – low, level 4 – medium and level 7 – high), resulting in a total of 28 cases summarized in Table 1. Reference cases refer to tests with only one fan running, while comparison cases refer to tests with both fans running.

Table 1. Experimental cases for double-fan interaction based on configurations shown in Figure 1A (O [0] – off, L [1] – low, M [4] – medium and H [7] – high fan speed level). Fan diameter *D* = 1.5 m.

Case #	Configuration 1 (1.3x*D*)		Case #	Configuration 2 (1.7x*D*)		Case #	Configuration 3 (2.1x*D*)	
	F1	F2		F2	F3		F1	F3
Reference cases								
1	O [0]	O [0]	1	O [0]	O [0]	1	O [0]	O [0]
2	L [1]	O [0]	11	L [1]	O [0]	20	O [0]	L [1]
3	M [4]	O [0]	12	M [4]	O [0]	21	O [0]	M [4]
4	H [7]	O [0]	13	H [7]	O [0]	22	O [0]	H [7]
Comparison Cases								
5	L [1]	L [1]	14	L [1]	L [1]	23	L [1]	L [1]
6	M [4]	L [1]	15	M [4]	L [1]	24	M [4]	L [1]
7	H [7]	L [1]	16	H [7]	L [1]	25	H [7]	L [1]
8	M [4]	M [4]	17	M [4]	M [4]	26	M [4]	M [4]
9	H [7]	M [4]	18	H [7]	M [4]	27	H [7]	M [4]
10	H [7]	H [7]	19	H [7]	H [7]	28	H [7]	H [7]

2.3 Air speed measurements

Figure 1 shows the grid of 180 measurement locations in the chambers (15 x 12 with 35-cm. spacing). The air speed was measured at each location at standardized heights of 0.1, 0.6, 1.1 and 1.7 m [25], resulting in a total of 720 measurement points per case. Totally 5,760 (720 × 8) and 20,160 (720 × 28) measurements were taken for single-fan and double-fan cases respectively. We used omnidirectional hot-wire anemometers (AirDistSys5000, Sensor Electronics, Poland), providing a measurement range from 0.05 m/s to 5 m/s with an accuracy of ±0.02 m/s ± 1.5% of readings. Reported values are means from 90 records measured in a sampling interval of 2 s (average of 3 min). 24 anemometers were installed on the measurement tree shown in Figure 2.

We prepared all contour graphs of constant air speed presented in the paper with MATLAB software. The data between measurement points were filled with the linear regression using the values recorded at nearby points.

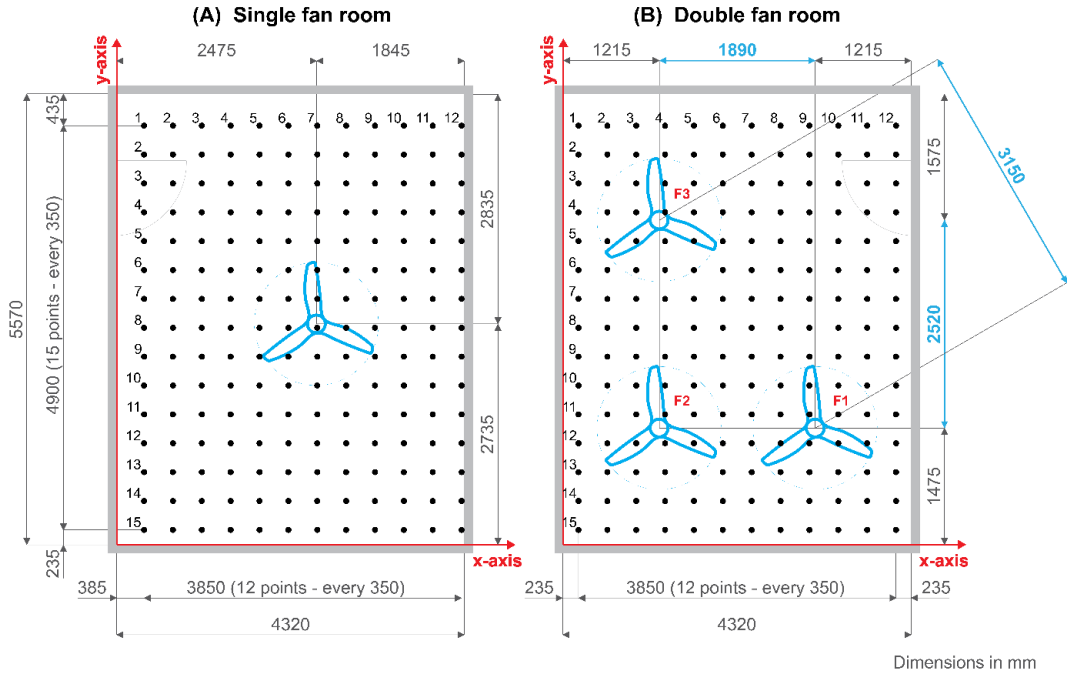

Figure 1. Measurement locations of air speed in climatic chambers: (A) single-fan room and (B) double-fan room.

Figure 2. Climatic chambers for air speed measurement: anemometer sensor tree.

3 Results

Due to the limited space, we visualize here only selected cases. The complete measurement results for all speed levels and other planes are available as CSV file in the Supplementary Information and visualized with the online tool (see Appendix B). The online tool, additionally to horizontal air speed contours at four planes (0.1, 0.6, 1.1 and 1.7 m above floor), visualizes the contour graphs for standing posture (average from 0.1, 1.1 and 1.7 m), sitting posture (0.1, 0.6 and 1.1 m) and average from all four heights. Air speed in the climatic chambers not generated by ceiling fans did not exceed 0.05 m/s.

3.1 Single-fan case

We can see from the cross-section view in Figure 3 that the fan propeller creates a ring jet seen as two cores (peak air speeds), a hollow in the center and a shear flow in the annular free-boundary layer along the jet. Regardless of the fan speed and orientation, cores are observed 0.35-0.4 m from the fan center (46-53% of the fan radius). Except for the low-speed level, the core-to-hollow difference is well defined within the whole jet depth down to the floor. At the low-speed, the jet has similar air speeds

across it (0.3-0.5 m/s) and terminates at 0.4-1.0 m above the floor. As shown in Figure 3B along x-axis and Figure 3C along y-axis, we did not obtain the ideally symmetric flow in cross-section views, which is characteristic for swirl flows [39], suggested by others [29,30]. This result shows also that fan jet is sensitive even to small room asymmetry and irregularities. Differences in the peak air speed values in cores along y-axis are in the range of 0.2-0.7 m/s and 0.2-0.4 m/s at heights of 1.1 m and 0.6 m respectively. Despite that, the general trend of flows is consistent with previous work [29,30].

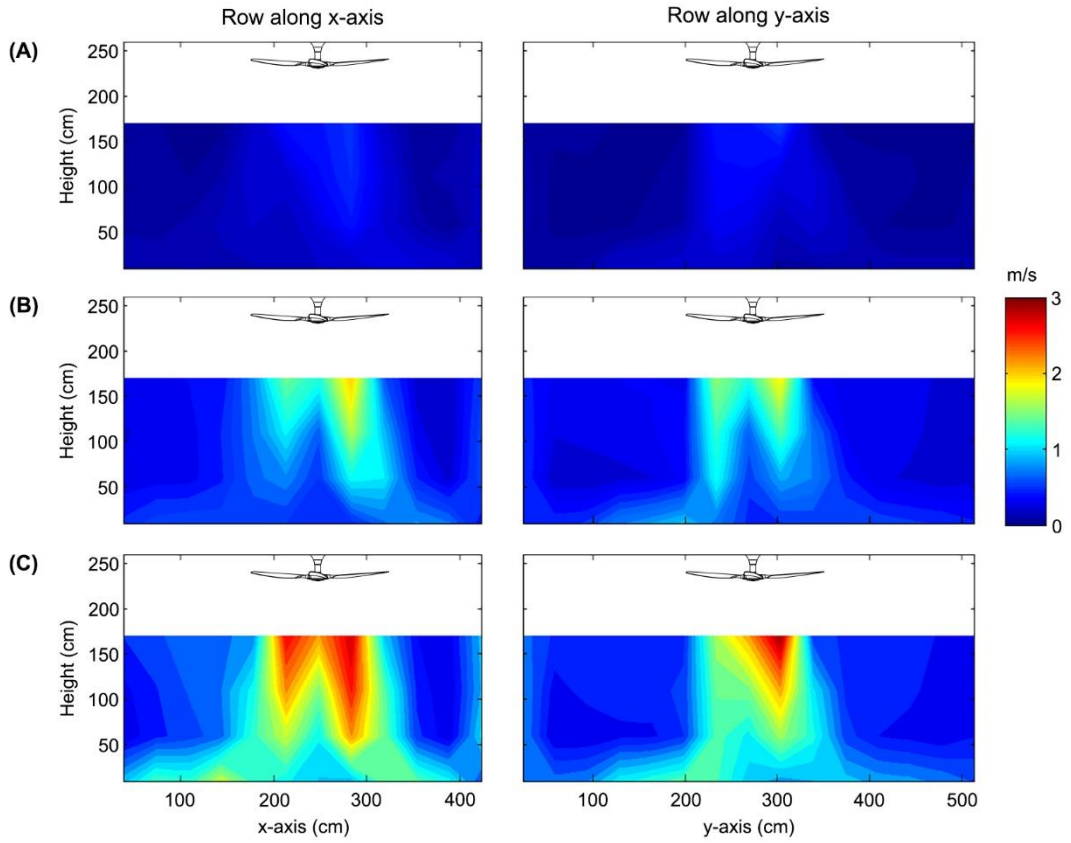

Figure 3. Vertical air speed contours on planes crossing the center of the ceiling fan (Row 8 and Column 7) with different speed levels: (A) low; (B) medium and (C) high.

The jet from the fan, in general, does not spread beyond the fan diameter until it passes through the height level of 0.8 m above the floor. With increasing fan speed level and air speed in the core, one sees increased induction of room air into the fan jet that intensifies air movement in most of the chamber. As shown in Figure 3 and Figure 4, air speeds equal to or higher than 0.2 m/s are measured directly below the fan at the low-speed level in the area within its perimeter until the jet starts spreading along the floor and affects 25% of the room area. When the fan is on medium speed, air speeds of 0.3 m/s or higher are observed in up to 1 m radial distance from the fan center (1.3x fan radius) and 1.5 m (2.0x fan radius) at the height of 1.1 m and 0.6 m respectively. Still air zones with air speed below 0.2 m/s are limited only to 5% of room area outside sheer flow along fan jet and walls, and heights between 0.6 m and 1.1 m. The affected room space is getting more prominent with the increase of fan speed level. No still air zones are identified in the occupied area when the fan is working at the highest speed level.

Below 0.6 m, the impact of the stagnation pressure can be observed in the decrease of air speed along the central streamline and the redirecting of the divided jet to be spread evenly along the floor. When reaching the wall, the airflow is redirected upwards along the wall.

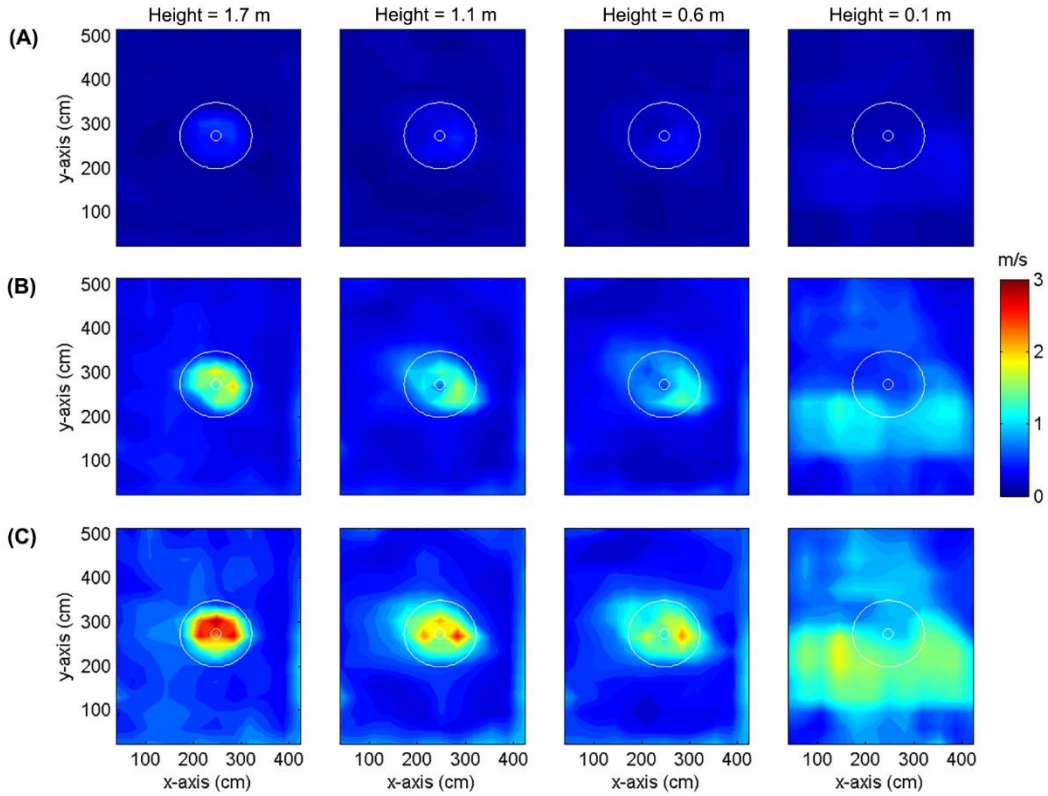

Figure 4. Horizontal air speed contours at four planes (0.1, 0.6, 1.1 and 1.7 m above floor) with different speed levels: (A) low; (B) medium and (C) high.

3.2 Double-fan case

All plane views for the double-fan scenario show mean air speeds calculated from measurements at heights of 0.1, 0.6, 1.1 and 1.7 m for each location. Measurements at each height and two different averaging approaches (seating and standing) can be seen in the online tool.

Figure 5 presents how the air speed changes for the Configuration 2 (Table 2) with a center-to-center distance of 1.7x*D* between the fans, with F2 set at medium speed throughout, and F3 changing through off-, low-, and medium-speed respectively. Compared to F2 operating alone (Figure 5A), the additional operation of F3 (Figure 5B and Figure 5C) strongly affects the air field below it and the air speed profile of F2. With the increased speed of F3, the joint airflow by F2 and F3 further encroaches into the still air zone. In Figure 5C with the medium speed of both F2 and F3, the two fans push the air towards each other and reach a balance in the middle area between the fans. The flow field of the two fans working together is not just the sum of the two. Therefore, we can deduce that when fans are close enough, we need to measure the air speed profile generated by the combination of the two, as their impact on occupants' comfort could be underestimated.

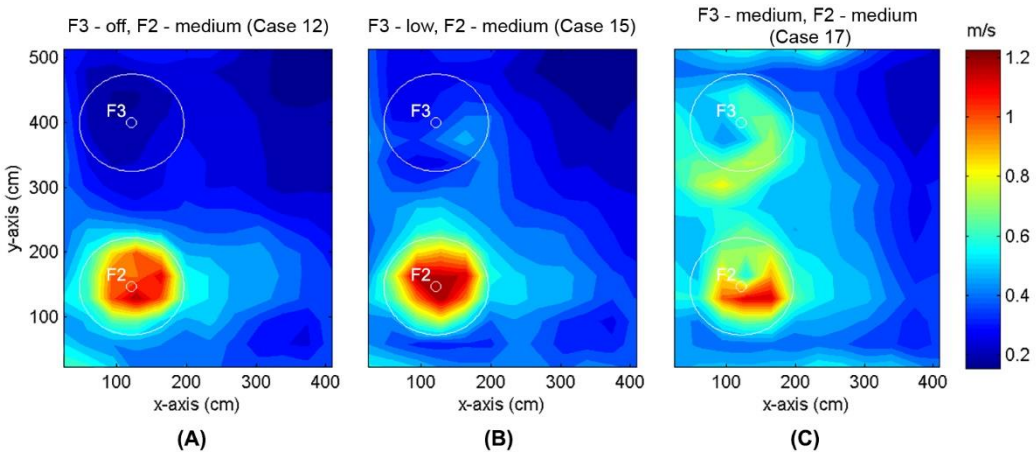

Figure 5. Average air speed (0.1, 0.6, 1.1 and 1.7 m height) in Configuration 2 (Table 2) as an example of the interaction of two fans (F3: upper position; F2: lower position, 1.7xD apart) with different combinations of speed levels: (A) F3 – off, F2 – medium (mirrored Case 3); (B) F3 – low, F2 – medium (Case 12) and (C) F3 – medium, F2 – medium (Case 14).

The distribution of the air speed generated by two fans operating at the same speed level is shown in Figure 6. It can be deduced from this figure that with the increased speed setting (from the 1st row to the 3rd row of the figure), more room area has average air speed higher than 0.5 m/s. When fans are set on medium speed level, regardless their configuration, more than 40% of the room is affected by air speed higher than 0.5 m/s. At high speed level, 70%, 80% and 100% of room area has average air speed above 0.5 m/s at Configuration 1 (center-to-center distance of 1.3x*D* along the shorter wall), Configuration 2 (1.7x*D* along the longer wall) and Configuration 3 (2.1x*D* along diagonal) respectively. We presume that differences at high speed are a result of the geometrical limitations of the test room.

The distance between two fans also has an observable influence on air speed values measured in the zone between fans. For distances of 1.3x*D* and 1.7x*D* shown in Figure 6A and Figure 6B respectively, we can see a substantial increase in the air speed in the middle area compared to surroundings. In the Configuration 3 (2.1x*D* distance between, Figure 6C), the air speed within the whole room increases substantially, while jet cores of each fan remain almost independent. Therefore, the influence of fans on each other in the middle zone at 2.1x*D* distance is not noticeable with this type of evaluation. We do not have enough data to conclude which is the distance that allows fans to act independently. This is worth further investigation in the future.

DOI: 10.1016/j.buildenv.2018.06.037
https://escholarship.org/uc/item/2mk3n264

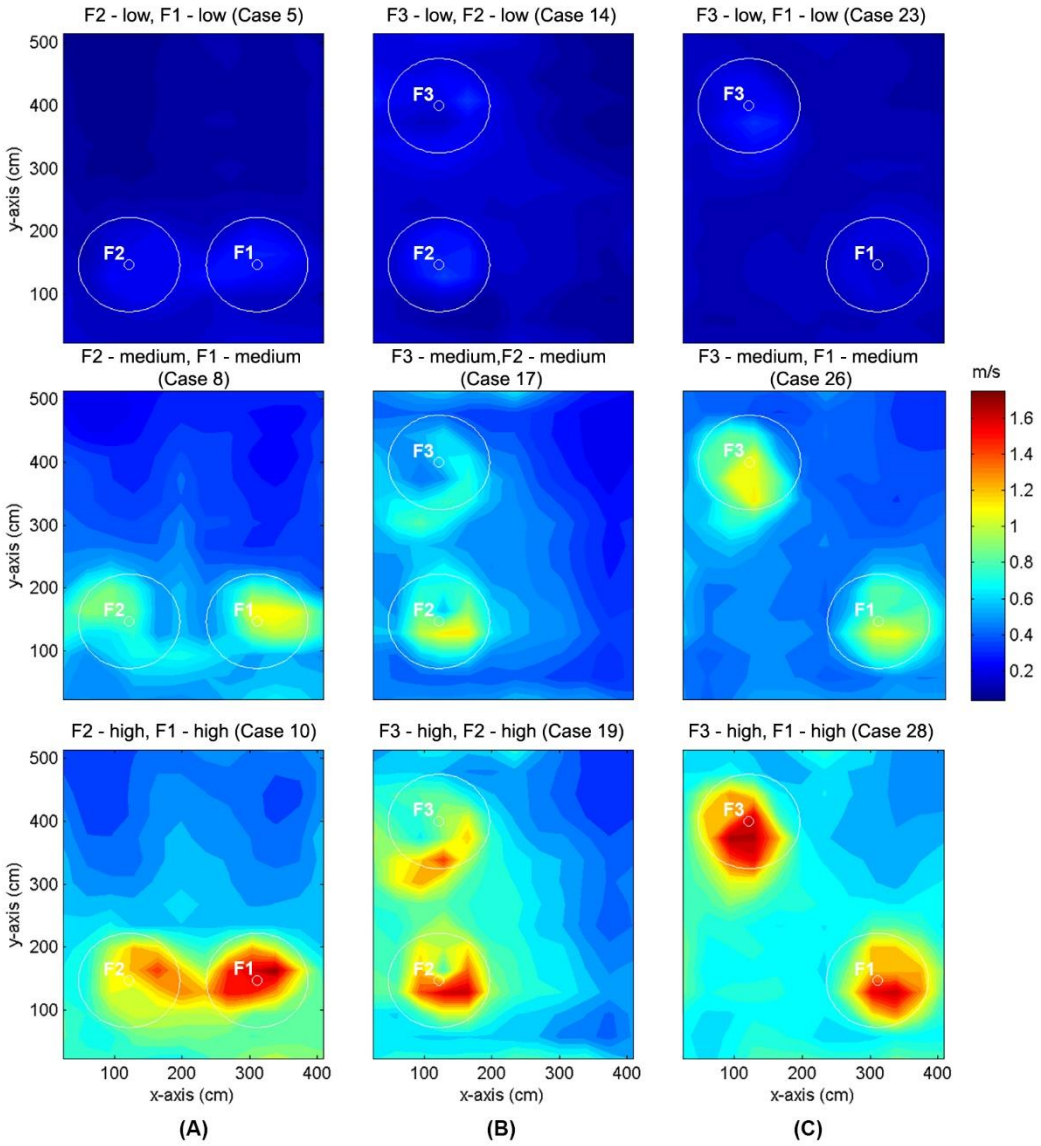

Figure 6. Air speed (m/s) contours (averaged on four horizontal planes) of two ceiling fans operating at the same speed level at different center-to-center distances: (A) 1.3xD; (B) 1.7xD and (C) 2.1xD.

This can be further seen via the cross-section view of vertical planes crossing the centers of two fans, as shown in Figure 7. The interaction of fan jets increases with the decrease of the distance between the fans. The gradient of speed in the boundary layer around the jet core in the middle area between fans is smaller at Configuration 2 (1.7x*D* distance) than at Configuration 3 and the singular-fan case, resulting in more uniform air speed values in this area. This suggests that fans should be installed closer to each other to achieve a more uniform distribution of air speed within the space between fans. Both jets have the most noticeable impact on each other at the shortest distance between fans (1.3x*D* distance, Configuration 1) and highest fan speed level (Case 10). Cores of both fan jets are directed to each other and from the height of 1.5 m down the boundary layers from both jets are joined in the middle zone between fans.

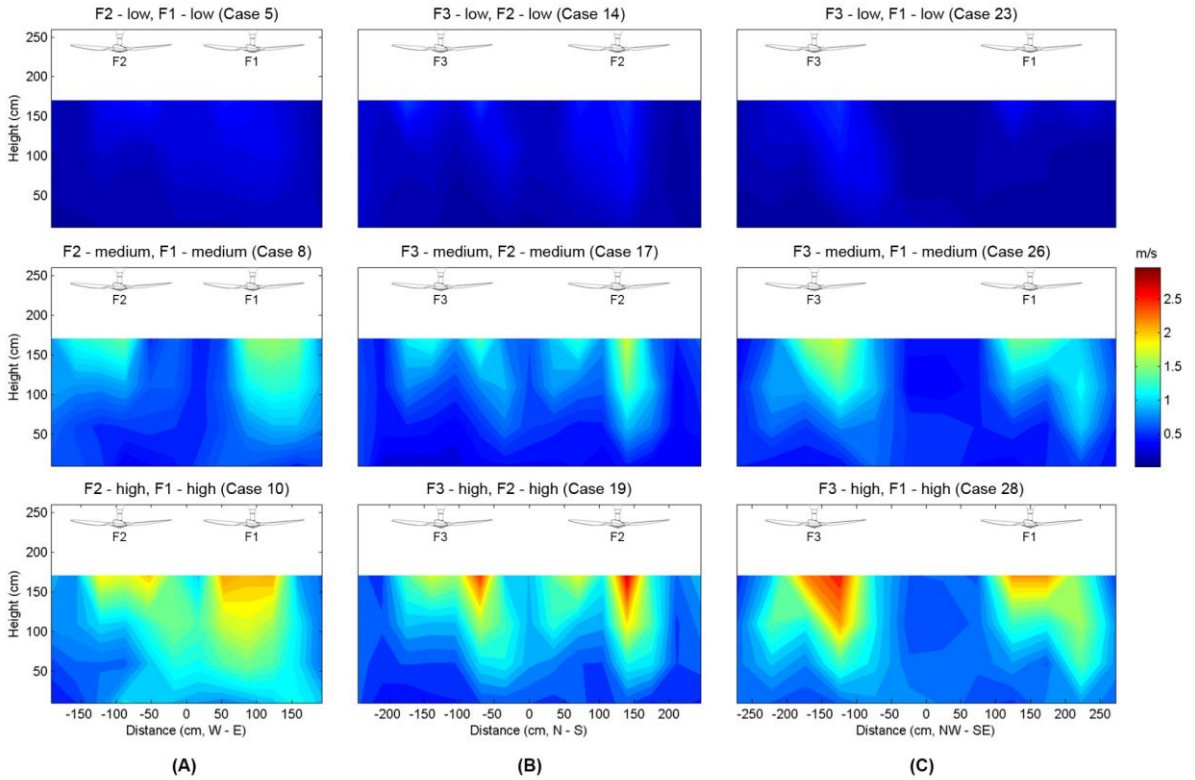

Figure 7. Air speed (m/s) contours (vertical plane crossing the centers of the fans) of two ceiling fans operating at the same speed level at different center-to-center distances: (A) 1.3x*D*; (B) 1.7x*D* and (C) 2.1x*D*.

The distribution of the average air speed generated by two fans operating at different speed levels is shown in Figure 8. Results show that a weaker fan set with a low-speed level has nearly no impact on the other regardless the distance between fans and the set point of the latter. Distributions of average air speed when the former fan is turned off (available in the online tool), and at low speed, are the same for all three configurations. When F1 is the stronger fan (Configuration 1 and 3), 16% and 32% of the room area has average air speed above 0.5 m/s at its medium speed (Cases 3, 6 and 24) and high speed (Cases 4, 7 and 25) respectively. Performance of F2 as the dominant fan at Configuration 2 is higher than F1 at Configuration 1 and 3: 18% of the room is affected by air speed higher than 0.5 m/s at its medium speed (Cases 12 and 15) and 52% at high speed (Cases 13 and 16).

If the weaker fan is set on the medium speed level, we can observe the increase of the fan interaction at short (1.3x*D*, Configuration 1) and middle (1.7x*D*, Configuration 2) distances between fans. The jet of the weaker fan (F2 at Case 9 and F3 at Case 18) is not symmetrical but skewed into the direction of the dominant fan, and the peak speed appeared at the fan edge. From this, we can conclude that fan speed affects the level of fan interaction.

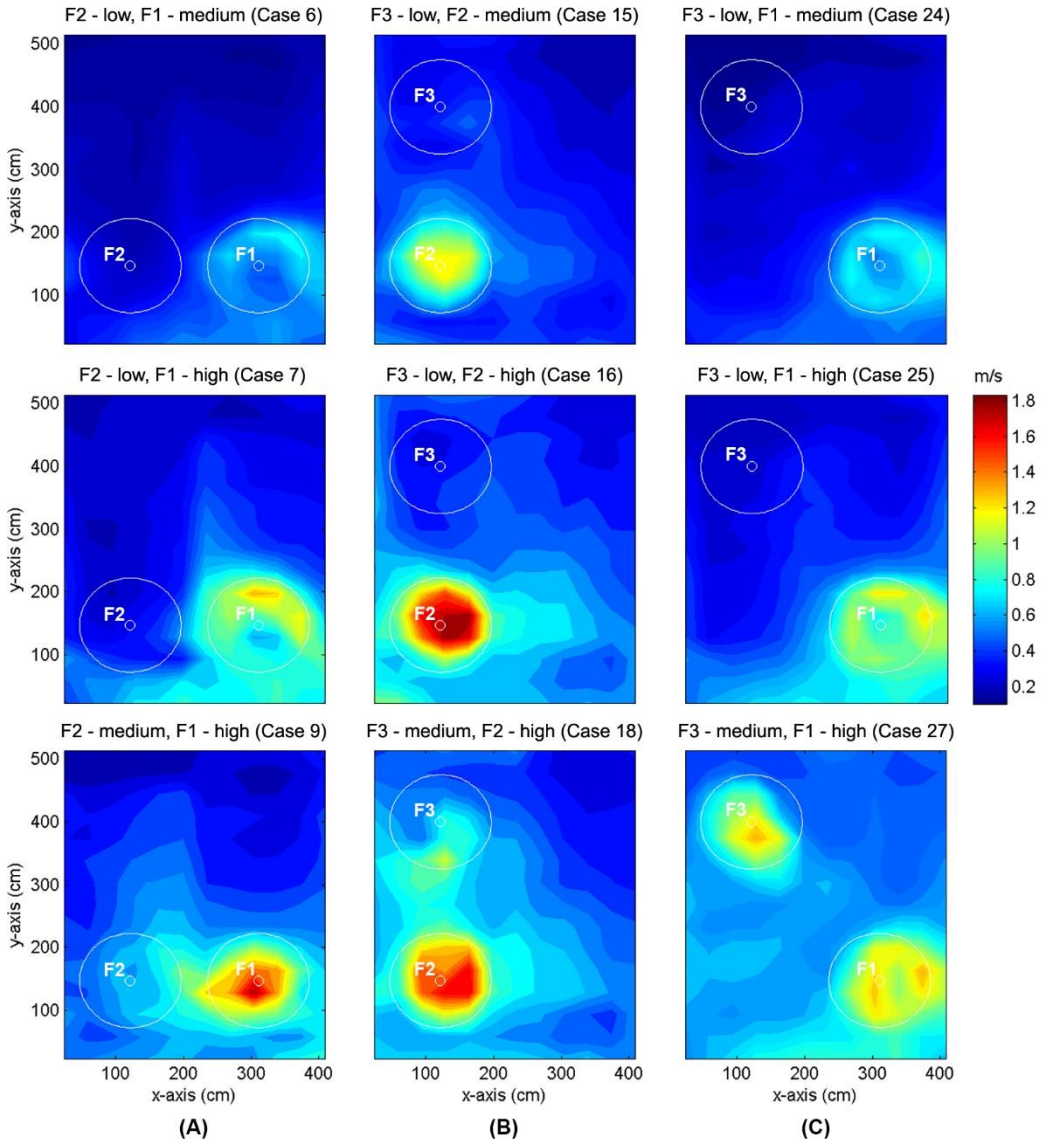

Figure 8. Air speed (m/s) contours (averaged on four horizontal planes) of two ceiling fans operating at different speed levels at various center-to-center distances: (A) 1.3xD; (B) 1.7xD and (C) 2.1xD.

Figure 9 shows the cross-section views for scenarios of fans working at different speed levels. It confirms that the impact of both fans on each other is much reduced at the longest center-to-center distance. We can observe that when the weaker fan is set at low speed, the change of speed level of the faster fan from medium to high affects the air speed magnitude but not the distribution pattern. However, when the speed level of the weaker fan increases from low to medium, the change in the air jet from the dominant fan (high-speed level) can be observed in Configurations 1 and 2. At the center-to-center distance of 1.7x*D* (Figure 9B), the width of the stronger fan jet together with boundary level increases by 20% at the height of 1.1 m, while the jet penetration decreases by 10-20 cm. At the same time, the jet of a weaker fan at the medium speed level penetrates up to 0.6 m above the floor even though it is skewed towards the stronger fan. The strongest interaction is observed at the shortest center-to-center distance (1.3x*D*, Figure 9A) when the stronger fan absorbed the air jet from the weaker one. As a result, the peak air speed in the core of the jet from the stronger fan increases by 0.5 m/s, the core becomes more focused and 40 cm longer.

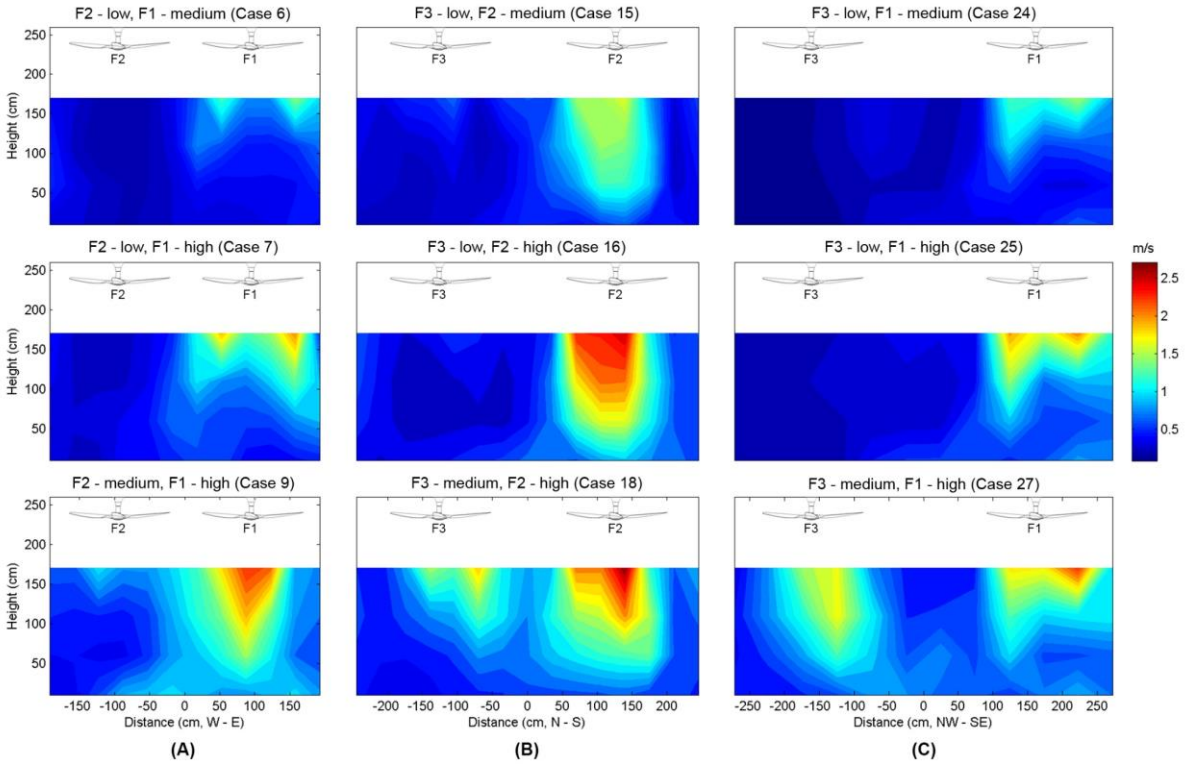

Figure 9. Air speed (m/s) contours (vertical plane crossing the centers of the fans) of two ceiling fans operating at different speed levels at various center-to-center distances: (A) 1.3x*D*; (B) 1.7x*D* and (C) 2.1x*D*.

4 Discussion

4.1 Room airflow patterns

The direct antecedent of this study is Gao et al. [30] which studied the effect of workstation furniture on room air flows from a single ceiling fan. A conceptual model simplifying fan air flows was proposed for design purposes, and comfort metrics were examined along with air speed profiles. The reference condition for the results was the flow of the fan in an empty room. The type of fan and instrumentation used was the same as in this study.

The current work is the first to study the interaction of multiple fans, in an empty room. Its reference condition is also the flow from a single fan in an empty room. The single-fan reference conditions from the two studies can therefore be compared. Also, the conceptual flow model offered in [30] can be tested and augmented.

Figure 3 in this paper can be compared with Fig. 5 in [30], showing the measured fluid dynamic features of the flow. Similarly, Figure 10 is comparable with Fig. 20 in [30], showing simplified schemes of the main room air circulation. In both study, the patterns and dimensions in these two studies are very similar to each other.

The measured data from both studies show more spreading of the downward jet below 0.5 m height than indicated in the cylinder shape in the conceptual model [30], but this is a quite local effect occurring between 0.6 and 0.3 m height and is affected by the fan speed level and distance between fan and wall. Both datasets show slightly greater spreading (10-20%) at higher fan speed levels. The conceptual model might be modified to account for this spreading in empty rooms. However, in both studies the downward fan jet showed asymmetry in its horizontal cross-section that appears to be due

to subtle non-uniformity in the test room surroundings. Such irregularity is probably inevitable in any realistic building situation, and places a practical limit on the predictive precision of design tools.

As illustrated in Figure 10, the airflow from the downward jet is redirected and spreads horizontally along the floor and then upwards along walls. It requires a minimum fan speed to establish the whole room circulation, above which the flow increases with fan speed. The width of the fan jet and the floor and wall circulation layers are similar regardless the fan speed level. We observe here that the distance between fan and wall affects the fan jet and the annular shear layer from a height of 0.8 m downwards. The fan jet becomes wider and horizontally longer toward the more distant wall. This effect has not been noted in [30] or previous studies.

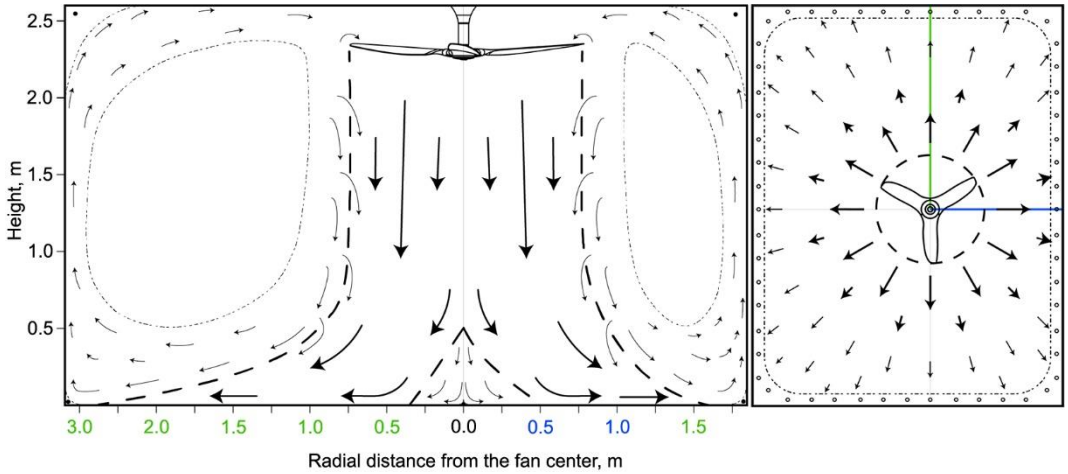

Figure 10. Air circulation in the single-fan room: cross-view across longest (green) and shortest (blue) distance to the wall (left) and plane view (right).

The use of two fans changes the behavior summarized in Figure 10. Figure 11 illustrates the air distribution when fans are at the closest distance (1.3x*D*). If both fans are set at medium or high speed (Figure 11A), both jets are skewed towards each other and join at the height of ~1.6 m, resulting in a high turbulence zone below the joining point. Air flow in this turbulent zone is directed towards the floor and horizontally towards walls or room space. Skewing of the jets also results in pushing stagnation points from directly below the fan centers to locations further from the middle point between fans. The boundary and room circulation layers are consistent with smoke visualization for the single fan. Due to the short distance between fan edges and walls, a zone of low-speed turbulences appears between the fan jet boundary and the layer of upward circulation along the wall. When both fans are set at low speed (Figure 11B), the smoke visualization shows that both jets are only slightly skewed towards each other, but become terminated at the height of 1.7 m. Beyond that, the smoke disperses within the room space. A similar termination height is observed for low-speed fan when the second fan is set at medium or high-speed level (Figure 11C). However, the jet from the weaker fan is strongly skewed towards the stronger fan. In addition, only the stronger fan influences the room air circulation: its jet drops and glides toward the floor below the weaker fan jet with a gentle slope. In addition, the air spreading along the ceiling above the weaker fan is directed toward the stronger fan instead of being sucked toward the weaker fan.

Figure 12 shows the air distribution at the middle center-to-center distance between fans (1.7x*D*). These results of smoke visualization are consistent with the results for the 2.1x*D* distance between fans. Therefore, we have omitted graphs for the Configuration 3. In general, both jets follow the

principle described for the single fan. The distance between fans affects the slope of the jet and boundary layers in the space between fans. Flows from both jets are joined at the middle point between the fans and directed upward. Low-speed turbulent zones appear between this upward joined flow and the boundary layers of both fans, similarly when the fan is located close to the wall. When both fans work at their low-speed level (Figure 12B), both jets are symmetric and terminate at the height of 1.5 m. When the speed of one fan is increased (Figure 12C), this fan dominates the room air circulation. However, it does not affect the performance of the weaker fan.

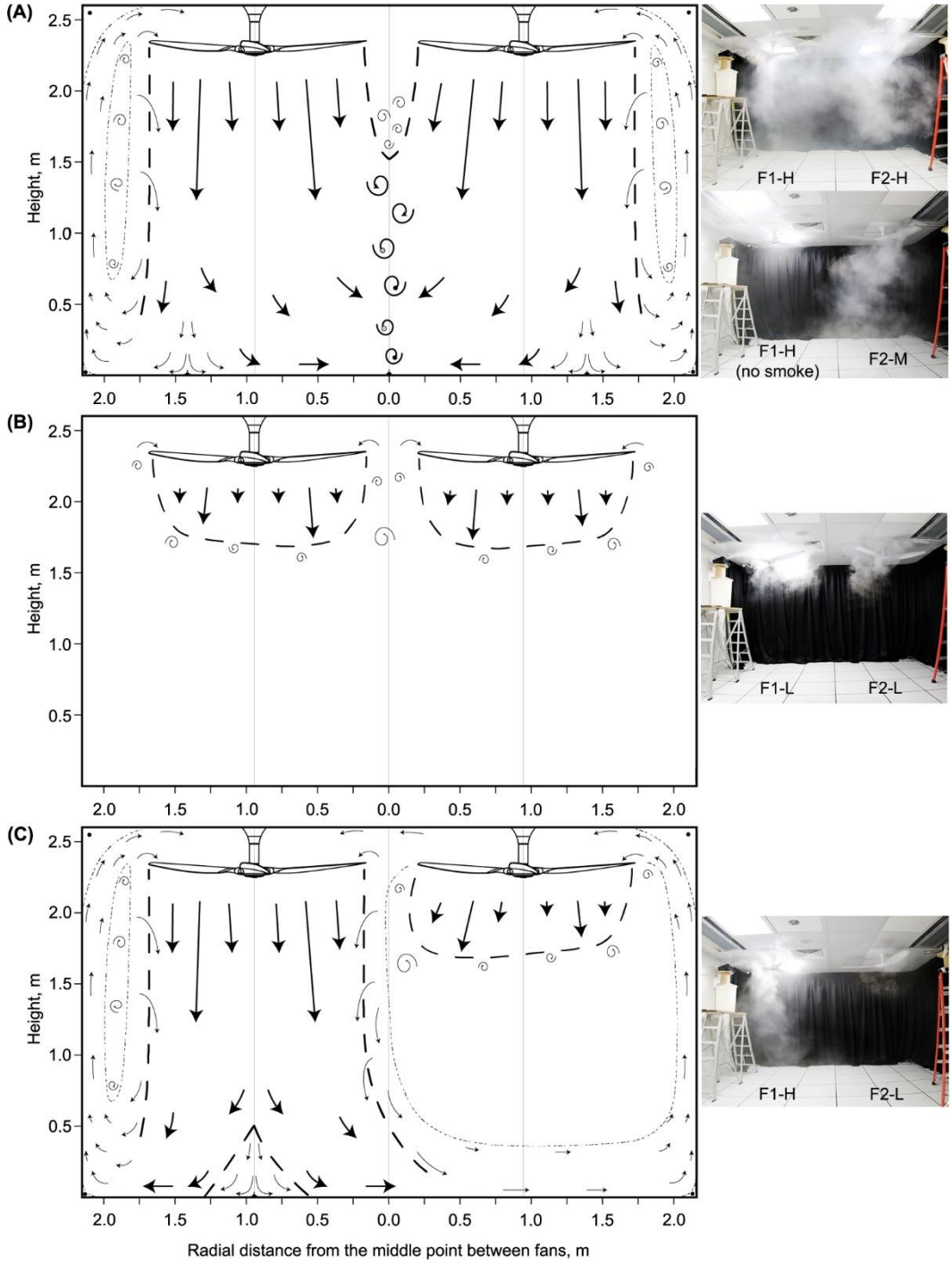

Figure 11. Air circulation in the double-fan room at the shorter center-to-center distance (1.3x*D*) – cross view at:
A) comparable scenario at medium-/high-speed levels (Case 8 M-M, Case 9 H-M and Case 10 H-H); B) comparable scenario at low-speed level (Case 5 L-L); C) dominant scenario (Case 6 M-L and Case 7 H-L).

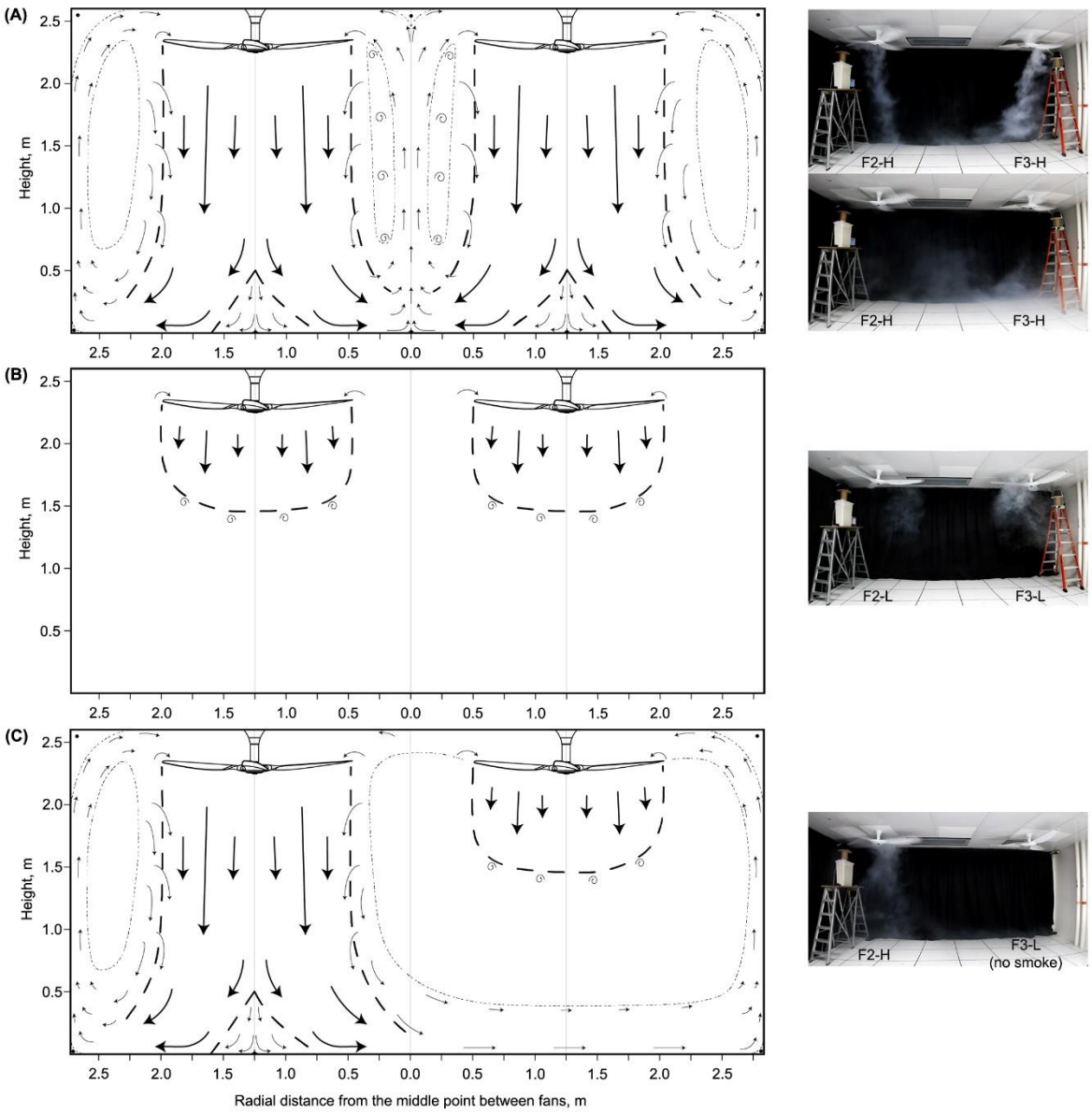

Figure 12. Air circulation in the double-fan room at the middle center-to-center distance (1.7x*D*) – cross view at: A) comparable scenario at medium-/high-speed level (Case 17 M-M, Case 18 H-M and Case 19 H-H); B) comparable scenario at low-speed level (Case 14 L-L); C) dominant scenario (Case 15 M-L and Case 16 H-L).

Plan views in Figure 13 illustrate how air spreading along the floor in the double-fan room depends on the fans' configuration. The upward flow along the walls appears in all study cases. When fans are installed along the shorter wall (Figure 13A), the jets turbulently join each other and define the longitudinal circulation loop within the room. Configuration 2, in contrast, results in a transverse circulation loop and increased upward flow in the middle zone between fans. Placement of fans according to Configuration 3 results in two separate triangular zones with the border along the room diagonal as shown in Figure 13C. If smoke is delivered to only one fan at this configuration, it remains in its zone for a substantial time, which indicates limited mixing in the border's upward flow zone. Figure 13C shows an example how the dominating fan defines the room air circulation when the weaker fan is set at low speed.

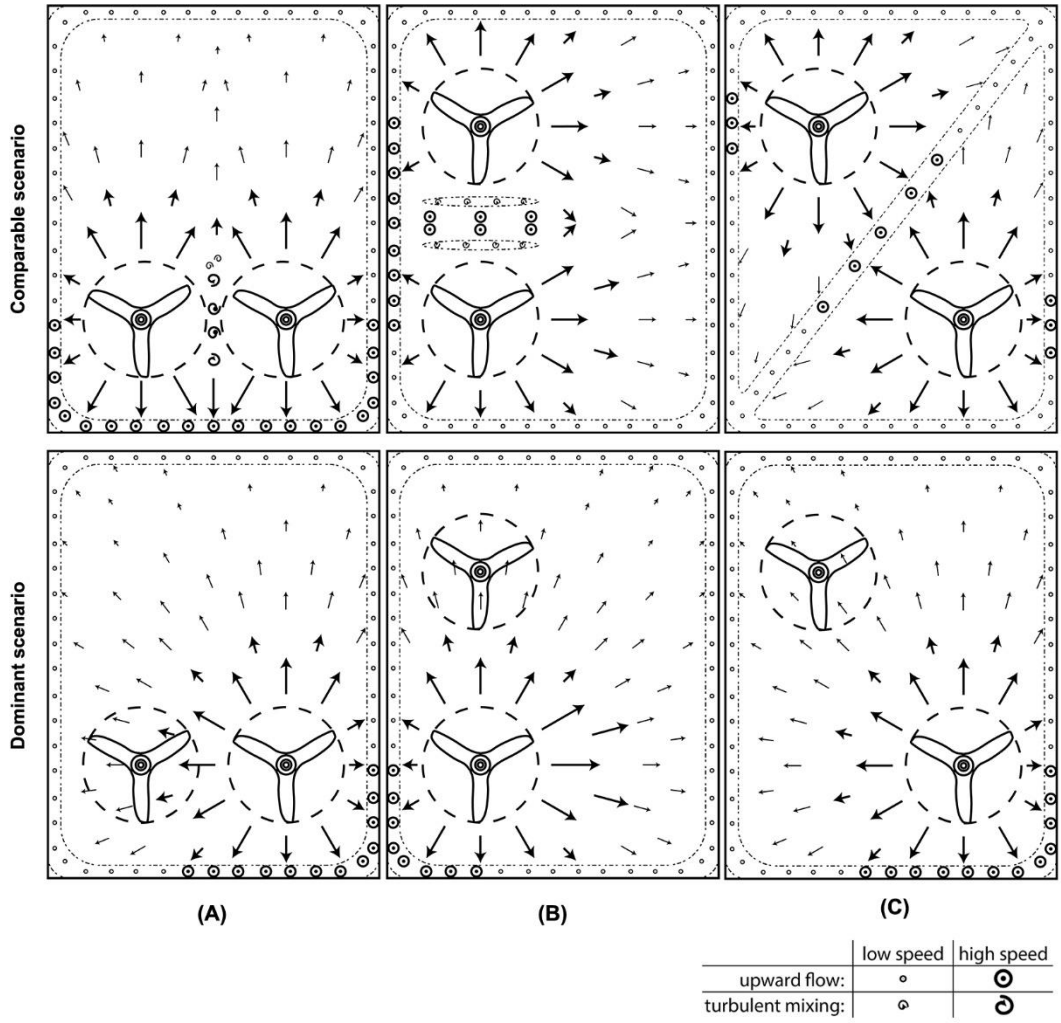

Figure 13. Air circulation in the double-fan room – plan views at the 0.5 m: (A) 1.3x*D*; (B) 1.7x*D* and (C) 2.1x*D*. Comparable scenario refers to cases when performance of both fans is relatively similar, while dominant scenario to cases when fan with higher speed level has a commanding position over the weaker fan.

The results show that use of multiple fans creates relatively uniform air speed profiles in the space, even though the air distribution (Figure 13) and character of the jets' interaction (Figure 11 and 12) slightly change depending on the fan configuration. At the shortest studied distance (1.3x*D*), the jets join each other and create a turbulent zone with relatively uniform air speed. On the other hand, the middle distance (1.7x*D*) appears to be short enough for the low-speed turbulent zone between downward jet flow and upward flow not to be substantial, which results in the relatively uniform air speed profile between fans. The assessment using the interactional speed ratio index (Appendix A) has the most relative effect between the fans. Gao et al. [30] showed that furniture redirect the jet's airflow laterally in a deeper spreading zone, therefore, we can suspect it will also increase the interaction level between the multiple fan jets. The air movement induced with multiple fans can then satisfy more occupants, even when they are not directly under the ceiling fan. Moreover, use of the multiple fans installed in the matrix instead of a single fan in bigger size allows for a cooperative control approach [38], which has the flexibility to adjust fans operation to occupants preferences and furtherly increases their satisfaction. It is possible that running the fans in reverse (moving the air toward the ceiling) may create an even more uniform environment.

4.2 Air Speed Ranges Coverage (ASRC) index for a ceiling fan

According to the ASHRAE 55 [25] and European standards [26,40], thermal comfort evaluations should be based on measurements performed at levels representing heights of ankles, abdomen and neck (0.1, 0.6 and 1.1 m for seated occupants, and 0.1, 1.1 and 1.7 m for standing occupants). Therefore, we identified the steady-state air distribution by averaging the air speed at the three heights at each measurement location for seated and standing occupants respectively, and assessed their impact on occupants' thermal comfort both visually and quantitatively. As shown in Figure 14 and Table 2, we evaluated the air speed distribution using the 0.2 to 0.8 m/s as effective air speed limits–the crucial thresholds to select different methods to determine the acceptable thermal environment in occupied spaces in accordance with ASHRAE 55 Standard [25]. If air speed is below 0.2 m/s, the graphic and analytical comfort zone methods are applicable; otherwise the elevated air speed comfort zone method is required. If there is an occupant control over the air speed, there is no upper air speed limit; otherwise the upper limit of air speed is 0.8 m/s. Standard [25] defines the occupant control as one means of control for every six occupants or less, or at least one control for each shared-activity common rooms.

We can observe patterns of average air speed distribution for seated occupants in Figure 14A. Profiles for standing occupant case are similar to seated scenario, therefore, we omit them in the paper and readers can access them through the online tool. The dark blue area in Figure 14A has the air speed lower than 0.2 m/s. It only appears when the fan is set at low speed, where the air speed is always below 0.8 m/s. The dark red part refers to the area with air speed larger than 0.8 m/s, which is not suitable for occupants without control over the fan speed. The dark red area is within the fan blade radius with medium speed. When fan is set at high-speed level, nearly one-third of the room is not suitable for occupants lacking control over the fan.

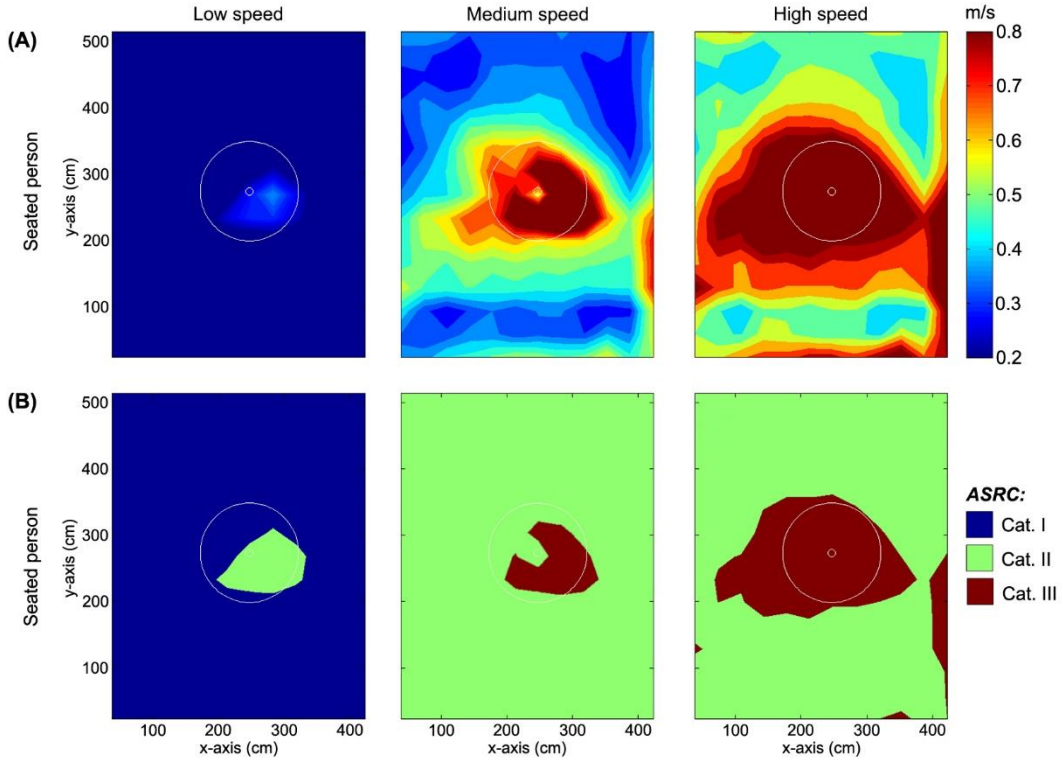

Figure 14. (A) Contours of air speed (m/s) averaged for seated occupants (0.1, 0.6 and 1.1 m) and (B) its categorical evaluation according to *ASRC*.

We propose an Air Speed Ranges Coverage (*ASRC*) to quantitatively assess the category of averaged air speed distribution induced by a ceiling fan in the room. The *ASRC* index is defined as the percentage of measurement locations (totally 12 × 15 = 180 locations for our study) in the space where the average air speed is within the specified category of air speed level:

I. less than 0.2 m/s,
II. larger than 0.2 m/s but less than 0.8 m/s, and
III. greater than 0.8 m/s.

For a specific fan speed level, we considered air speed (v_a) on specific heights for seated and standing occupants respectively. Figure 14B shows air speed values classified according to the above criteria.

Table 2. Air Speed Ranges Coverage (*ASRC*) of a ceiling fan for seated and standing occupants. Bold font indicates the dominant air speed category.

Fan speed level	Power (W)	RPM	*ASRC* – seated person (%)			*ASRC* – standing person (%)		
			Cat. I	Cat. II	Cat. III	Cat. I	Cat. II	Cat. III
			v_a ≤ 0.2 m/s	0.2 m/s < v_a ≤ 0.8 m/s	v_a > 0.8 m/s	v_a ≤ 0.2 m/s	0.2 m/s < v_a ≤ 0.8 m/s	v_a > 0.8 m/s
1	2	36	**94**	6	0	**93**	7	0
2	4	71	31	**69**	0	28	**71**	1
3	5	86	4	**95**	1	4	**93**	3
4	9	122	0	**95**	5	0	**94**	6
5	17	157	0	**85**	15	0	**88**	12
6	20	166	0	**79**	21	0	**83**	17
7	23	176	0	**73**	27	0	**74**	26

As shown in Table 2, the difference in the *ASRC* between seated and standing positions is not substantial. The index for Category I (v_a ≤ 0.2 m/s) drops dramatically from about 94% with the increase of fan speed until it reaches zero when the set-point equals to level 4. Such trend is expected as the main function of a ceiling fan is to provide increased air movement. We can see that the average air speed at most of the tested locations is in the range from 0.2 m/s to 0.8 m/s (Category II) with fan speed level 2 or above. With increased fan speed, the index in air speed Category II increases first and reaches the peak (93% ~ 95%) with the fan speed level 3 or 4, and then decreases due to increasing percentage of room area with air speed in Category III (> 0.8 m/s). Category III is acceptable if there is personal control of the fan. The maximum values for Category III reach 27% and 26% for seated and standing occupants respectively at the highest fan speed (level 7). The *ASRC* index is useful for having an assessment of how much of the area is covered by the fan usable air speed.

4.3 Density of measurement points

Most studies of air speed fields below ceiling fan have performed measurements in a single line with different radial distances starting from the fan center [29,31–33,35]. However, the flow below the fan is highly unsteady—air speed changes in time reflecting highly turbulent flow. Measurements show differences of up to 0.7 m/s in the peak air speed values between two sides of the fan at the height of 1.1 m even though distances to the opposite walls are balanced (Figure 3). This suggests that

measurements performed in a single radial measurement line may underestimate or overestimate the air speed, and therefore the fan performance and its impact on occupants' comfort. To study this further, we conducted additional measurements for a single fan at medium speed level adopting methodology given in ASHRAE 216P [35]–a new ASHRAE Standard on the performance of ceiling fans, which is still under development. The current state of the standard requires tests of ceiling fans in a singular line from the fan center to a room corner, with the fan installed centrally in the square room. Distances between test positions should be consistent from fan center (Test Position 0 – TP_0) to the radius of the fan size (r), from r to a distance twice the radius of the fan ($2r$) and from $2r$ to the corner of the room (furthest point to be placed 60 cm from the corner, TP_{max}). The increments are depended on the fan size. Additional measuring point should be placed at the $2.5r$ distance from the fan center. The measurements to calculate the average air speed should be taken each 2 s for a sampling time increasing in 180-second increments until steady state conditions are achieved, up to a maximum of 12 min, at which steady state conditions are assumed to be met. All measurements need to be done without any background air flow and heat sources placed in the test room, and with a fan working for at least 15 min at tested speed set point.

We were not able to install a fan in the central location on the x-axis due to obstructions and the rectangular dimensions of our test room (5.6 × 4.3 m). Therefore we measured air speed profiles in the radial lines from fan center to each corner and to each wall as shown in Figure 15A. Results in Figure 15B are grouped according to congruent distances (L1-L5, L6-L8 and L2-L4) and remaining pair (L3-L7).

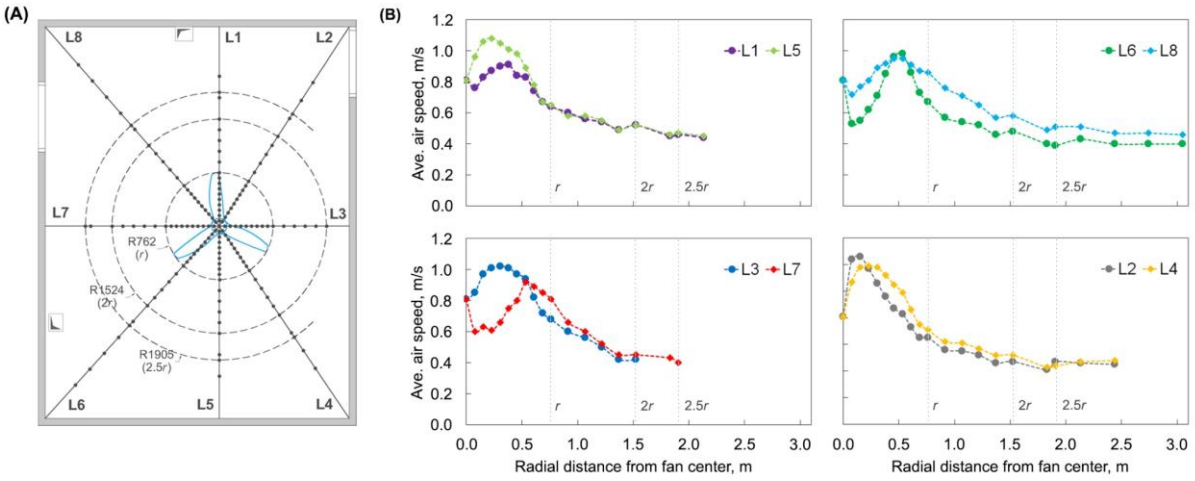

Figure 15. Air speed measurements in radial lines: (A) measurement points in radial distances according to ASHRAE 216P [35]–every 3 in. (7.6 cm) within the fan radius (r), every 6 in. (15.2 cm) within $2r$ range and every 12 in. (30.5 cm) further from the fan; (B) radial profiles of air speed averaged for seated occupants (0.1, 0.6 and 1.1 m) at medium fan speed level (level 4)–grouped according to congruent distances to walls/corners.

The highest difference in the zone below the fan is observed along the axis along which the fan is not centered (L3-L7)–the average air speed for seated occupant is 0.4 m/s (0.5 m/s for standing) higher at the shorter distance to the wall. After the $1.5r$ radial distance, the differences in average air speed are negligible. The substantial differences are observed between measurement lines L6 and L8 (the longest measurement lines), where air speed is equal at the peak, but the difference of 0.2 m/s has been recorded at the remaining part of the jet core and sheer flow until the $1.5r$ radial distance from the fan center. Afterwards, the difference of 0.1 m/s is observed until the last measurement point. For a standing person scenario, the differences between L6 and L8 reach 0.4 m/s. For the remaining

congruent measuring lines (L1-L5 and L2-L4), the differences of 0.2 m/s are observed in the jest core and are negligible afterwards.

The ASHRAE 216P [35] gives a methodology for calculating a weighted average of room air speed and cooling effect (*CE*, based on the change in Standard Effective Temperature (SET) [25]). The ASHRAE 216P [35] also defines the Cooling Coverage Fraction (*CC*) as a fraction of points where average air speed for seated and standing occupants respectively is equal or greater than 0.43 m/s (85 fpm), which results in *CE* of 2.2 °C (4 °F). All used equations are included in Appendix C. Table 3 summarizes room average assessment for each measurement lines. As the weighting factors increase with the radial distance from the fan center, the differences in the main fan jet described above are not reflected in the room average values. The average cooling effect in the zone below the fan (*r*) is ~1 °C higher than room average, whereas differences in *CE* at the same radial distances of congruent lines L6 and L8 reach up to 0.5 °C and 0.8 °C for seated and standing occupant respectively. Therefore, we recommend that more tests in larger rooms should be done to verify if more than one direction should be measured. It seems that higher spatial resolution measurements is needed in the area below the fan.

The *CC* calculated for congruent lines L6 and L8 shows substantial differences between those lines. For a reference, the *CC* calculated based on high spatial measurements described in Section 3.1 for the medium fan speed is 47% for seated occupants and 46% for standing. Only *CC* calculated for L6 is within 10% difference compared to reference values from high spatial measurements. This suggests that *CC* value can be strongly biased if only one radial measurement line is used. The simplified measurements along one radial line can be used for fast comparison of the fan impact on the whole room using the room average air speed and *CE*.

Table 3. Room average air speed, Cooling Effect (*CE*) and Cooling Coverage Fraction (*CC*) for seated and standing occupants respectively [35].

Radial line	L1	L5	L2	L4	L8	L6	L7*	L3*
$v_{a,seated,room}$, m/s	0.54	0.55	0.51	0.55	0.55	0.46	0.55*	0.60*
$v_{a,standing,room}$, m/s	0.52	0.58	0.50	0.55	0.53	0.47	0.59*	0.59*
$CE_{a,seated,room}$, °C	2.5	2.5	2.4	2.5	2.5	2.2	2.5*	2.6*
$CE_{a,standing,room}$, °C	2.4	2.6	2.4	2.5	2.4	2.2	2.6*	2.5*
CC_{seated}, %	100	100	89	100	100	43	96*	72*
$CC_{standing}$, %	100	100	77	100	100	56	100*	72*

* Values for horizontally not centered axis.

Previous work [29] defined a model in which ceiling fans (in the single empty-room case) have negligible impact on the air speed in the zone outside the main fan jet (termed the 'still air zone') and spreading flows on floor and walls. The spreading flow zones can be thickened in various ways to 'eat into' the still air zones and provide more cooling. This occurs with the introduction of furniture surfaces above floor level and other obstructions like partitions on the floor, increased fan speed levels, and the collision of air jets from multiple fans which redirect flows upward as shown in [30] and here. Our experiments with two fans confirmed the conceptual model for multiple fans in [30] that the air speed within the room space increases as spreading zones collide. Beyond the conceptual model in [30], results showed interactions between multiple fans that are complex and might require

further measurements including combined effects of all fans. In fan testing protocols, measurements should be best performed within a whole test room or at least in a multiple radial lines.

4.4 Limitations and future work

We conducted air speed measurement in climatic chambers with limited dimensions which may result in asymmetrical results and with fans that were quite closely located (1.3xD ~ 2.1xD distances between fans). This could be improved in the future by introducing measurements in a more general open space with symmetrical fan locations. We are also interested in the effect of obstacles on the interaction among multiple fans.

5 Conclusion

We performed high-resolution air speed measurements for single-fan and double-fan cases (5,769 and 20,160 measuring points respectively) and smoke visualizations. We developed useful airflow patterns for fan manufacturers, designers and researchers to improve the location of fans. These measurements can be used to calibrate CFD simulation models.

The current study, both air speed measurements and smoke visualization for a single fan, confirmed the constancy of fan jet shape at different fan speeds. With increased fan speed, the still-air zone is reduced and the depth of jet core extends, resulting in stronger impingement of airflow towards the floor and improvement in the acceleration of circulation process. For the multiple-fan case, both the speed difference and the distance between the fans will affect the airflow profiles of each other. Therefore, when fans are close enough, we need to measure the air speed profile generated by the combination of the two.

The present study led to development of general patterns of room air flow circulation driven by single and multiple ceiling fans. These complement previous results in [30] derived from independent experiments.

We present airflow profiles of ceiling fans in the occupied zone using a newly developed mathematical index. The Air Speed Ranges Coverage (*ASRC*) index is defined as the percentage of measurement locations in the space in which the average air speed is within the specified limits of air speed. The limits are based on the ASHRAE thermal comfort standard [25]. It allows one to assess how much of the floor area is covered at a given effective air speed range.

We also develop an interactional speed ratio (*ISR*) index to quantify the relative effect of one fan on the other. We assessed the effect on the index of different fan speeds and distance between fans (see Appendix A).

Differences found in measurements taken along the eight radial axes from the center of the fan jet indicate that measuring along a single radial line may not be sufficient for proper evaluation of the airspeed mainly below the fan. Additional measurement points may be needed.

We finally present an online visualization tool with user-friendly UI (see Appendix B) based on all the measurement results. We believe this is a useful tool which greatly benefits the research community.

Acknowledgments

This research was funded by the Republic of Singapore's National Research Foundation through a grant to the Berkeley Education Alliance for Research in Singapore (BEARS) for the Singapore-

Berkeley Building Efficiency and Sustainability in the Tropics (SinBerBEST) Program. BEARS has been established by the University of California, Berkeley as a centre for intellectual excellence in research and education in Singapore.

References

[1] C. Duarte, P. Raftery, S. Schiavon, Development of whole-building energy models for detailed energy insights of a large office building with Green Certification rating in Singapore, Energy Technol. 5 (2017) 1–11. doi:10.1002/ente.201700564.

[2] T. Hoyt, E. Arens, H. Zhang, Extending air temperature setpoints: Simulated energy savings and design considerations for new and retrofit buildings, Build. Environ. 88 (2015) 89–96. doi:10.1016/j.buildenv.2014.09.010.

[3] S. Schiavon, A. Melikov, Energy saving and improved comfort by increased air movement, Energy Build. 40 (2008) 1954–1960. doi:10.1016/j.enbuild.2008.05.001.

[4] S. Sekhar, Higher space temperatures and better thermal comfort - a tropical analysis, Energy Build. 23 (1995) 63–70. doi:10.1016/0378-7788(95)00932-N.

[5] Z. Xu, S. Liu, G. Hu, C.J. Spanos, Optimal coordination of air conditioning system and personal fans for building energy efficiency improvement, Energy Build. 141 (2017) 308–320. doi:10.1016/j.enbuild.2017.02.051.

[6] S. Liu, L. Yin, W.K. Ho, K.V. Ling, S. Schiavon, A tracking cooling fan using geofence and camera-based indoor localization, Build. Environ. 114 (2017) 36–44. doi:10.1016/j.buildenv.2016.11.047.

[7] S. Schiavon, B. Yang, Y. Donner, V.W.-C. Chang, W.W. Nazaroff, Thermal comfort, perceived air quality and cognitive performance when personally controlled air movement is used by tropically acclimatized persons, Indoor Air. 27 (2017) 690–702. doi:10.1111/ina.12352.

[8] B. Yang, S. Schiavon, C. Sekhar, D. Cheong, K.W. Tham, W.W. Nazaroff, Cooling efficiency of a brushless direct current stand fan, Build. Environ. (2015) 196–204. doi:10.1016/j.buildenv.2014.11.032.

[9] Y. Zhai, H. Zhang, Y. Zhang, W. Pasut, E. Arens, Q. Meng, Comfort under personally controlled air movement in warm and humid environments, Build. Environ. 65 (2013) 109–117. doi:10.1016/j.buildenv.2013.03.022.

[10] E. Arens, T. Xu, K. Miura, Z. Hui, M. Fountain, F. Bauman, A study of occupant cooling by personally controlled air movement, Energy Build. 27 (1998) 45–59. doi:10.1016/S0378-7788(97)00025-X.

[11] Y. Zhai, E. Arens, K. Elsworth, H. Zhang, Selecting air speeds for cooling at sedentary and non-sedentary office activity levels, Build. Environ. 122 (2017) 247–257. doi:10.1016/j.buildenv.2017.06.027.

[12] J. Sonne, D. Parker, Measured ceiling fan performance and usage patterns: implications for efficiency and comfort improvement, in: Pacific Grove, CA, 1998: pp. 335–341.

[13] W. Oh, S. Kato, The effect of airspeed and wind direction on human's thermal conditions and air distribution around the body, Build. Environ. 141 (2018) 103–116. doi:10.1016/j.buildenv.2018.05.052.

[14] S.H. Ho, L. Rosario, M.M. Rahman, Thermal comfort enhancement by using a ceiling fan, Appl. Therm. Eng. 29 (2009) 1648–1656. doi:10.1016/j.applthermaleng.2008.07.015.

[15] M. Alizadeh, S.M. Sadrameli, Numerical modeling and optimization of thermal comfort in building: Central composite design and CFD simulation, Energy Build. 164 (2018) 187–202. doi:10.1016/j.enbuild.2018.01.006.

[16] A. Lipczynska, S. Schiavon, L.T. Graham, Thermal comfort and self-reported productivity in an office with ceiling fans in the tropics, Build. Environ. 135 (2018) 202–212. doi:https://doi.org/10.1016/j.buildenv.2018.03.013.

[17] A. Melikov, J. Kaczmarczyk, Air movement and perceived air quality, Build. Environ. 47 (2012) 400–409. doi:10.1016/j.buildenv.2011.06.017.

[18] F.H. Rohles, S.A. Konz, B.W. Jones, Ceiling fans as extenders of the summer comfort envelope, ASHRAE Trans. 89 (1983) 245–263.

[19] Y. Zhai, Y. Zhang, H. Zhang, W. Pasut, E. Arens, Q. Meng, Human comfort and perceived air quality in warm and humid environments with ceiling fans, Build. Environ. 90 (2015) 178–185. doi:10.1016/j.buildenv.2015.04.003.

[20] L. Huang, Q. Ouyang, Y. Zhu, L. Jiang, A study about the demand for air movement in warm environment, Build. Environ. 61 (2013) 27–33. doi:10.1016/j.buildenv.2012.12.002.

[21] J. Toftum, Air movement – good or bad?, Indoor Air. 14 (2004) 40–45. doi:10.1111/j.1600-0668.2004.00271.x.

[22] H. Zhang, E. Arens, S.A. Fard, C. Huizenga, G. Paliaga, G. Brager, L. Zagreus, Air movement preferences observed in office buildings, Int. J. Biometeorol. 51 (2007) 349–360. doi:10.1007/s00484-006-0079-y.

[23] G. Brager, G. Paliaga, R. de Dear, Operable windows, personal control and occupant comfort., ASHRAE Trans. 110 (2004) 17–35.

[24] E. Arens, S. Turner, H. Zhang, G. Paliaga, Moving air for comfort, ASHRAE J. 51 (2009) 8–18.

[25] A. 55, Thermal environmental conditions for human occupancy, American Society of Heating, Refrigerating and Air-Conditioning Engineers, Inc., Atlanta, GA, 2017.

[26] EN 15251, Indoor environmental input parameters for design and assessment of energy performance of buildings addressing indoor air quality, thermal environment, lighting and acoustics, European Committee for Standardization, Brussels, Belgium, 2007.

[27] SS 553, Code of practice for air-conditioning and mechanical ventilation in buildings, Building and Construction Standards Committee, SPRING Singapore, Singapore, 2016.

[28] D.S. Parker, M.P. Callahan, J.K. Sonne, G.H. Su, Development of a high efficiency ceiling fan. The Gossamer Wind, Florida Energy Office, Department of Community Affairs, Tallahassee, FL, 1999.

[29] A. Jain, R.R. Upadhyay, S. Chandra, M. Saini, S. Kale, Experimental investigation of the flow field of a ceiling fan, in: Charlotte, North Carolina USA, 2004: pp. 93–99. doi:http://dx.doi.org/10.1115/HT-FED2004-56226.

[30] Y. Gao, H. Zhang, E. Arens, E. Present, B. Ning, Y. Zhai, J. Pantelic, M. Luo, L. Zhao, P. Raftery, S. Liu, Ceiling fan air speeds around desks and office partitions, Build. Environ. (2017). doi:10.1016/j.buildenv.2017.08.029.

[31] W. Chen, S. Liu, Y. Gao, H. Zhang, E. Arens, L. Zhao, J. Liu, Experimental and numerical investigations of indoor air movement distribution with an office ceiling fan, Build. Environ. 130 (2018) 14–26. doi:10.1016/j.buildenv.2017.12.016.

[32] F. Babich, M. Cook, D. Loveday, R. Rawal, Y. Shukla, Transient three-dimensional CFD modelling of ceiling fans, Build. Environ. 123 (2017) 37–49. doi:10.1016/j.buildenv.2017.06.039.

[33] Y. Momoi, K. Sagara, T. Yamanaka, H. Kotani, Modeling of ceiling fan based on velocity measurement for CFD simulation of airflow in large room, in: Coimbra, Portugal, 2004: pp. 145–150.

[34] R. Aynsley, Fan Size and Energy Efficiency, Int. J. Vent. 1 (2002) 33–38. doi:10.1080/14733315.2002.11683619.

[35] A. 216P, Methods of Test for Determining Application Data of Overhead Circulator Fans, American Society of Heating, Refrigerating and Air-Conditioning Engineers, Inc., Atlanta, GA, 2018.

[36] S. Zhu, J. Srebric, S.N. Rudnick, R.L. Vincent, E.A. Nardell, Numerical modeling of indoor environment with a ceiling fan and an upper-room ultraviolet germicidal irradiation system, Build. Environ. 72 (2014) 116–124. doi:10.1016/j.buildenv.2013.10.019.

[37] R. Bassiouny, N.S. Korah, Studying the features of air flow induced by a room ceiling-fan, Energy Build. 43 (2011) 1913–1918. doi:10.1016/j.enbuild.2011.03.034.

[38] S. Liu, L. Yin, S. Schiavon, W.K. Ho, K.V. Ling, Coordinate control of air movement for optimal thermal comfort, Sci. Technol. Built Environ. 0 (2018) 1–11. doi:10.1080/23744731.2018.1452508.

[39] K. Oberleithner, C.O. Paschereit, J. Soria, Stability Analysis of Time-averaged Jet Flows: Fundamentals and Application, Procedia IUTAM. 14 (2015) 141–146. doi:10.1016/j.piutam.2015.03.034.

[40] 7726, Ergonomics of the thermal environment. Instruments for measuring physical quantities, European Committee for Standardization, 2001.

Appendix A. Interactional speed ratio (*ISR*) index between two ceiling fans

In Result section 3.2 and Discussion 4.1, we drew rough pictures on the absolute interaction between two fans by air speed measurements and smoke visualizations. However, we still lack tools to provide fine-grained analysis. To achieve this goal, we developed a mathematical index to quantify the relative effect from one fan on the other. Due to physical layout limitations, we only consider measurement locations in the area of directly affected by two fans (red blocks in Figure A.1) for a fair comparison. To minimize the influence from walls on the measured air speed, we did not select measuring points close to walls. At each measurement location, we used data measured at four heights (0.1, 0.6, 1.1 and 1.7 m).

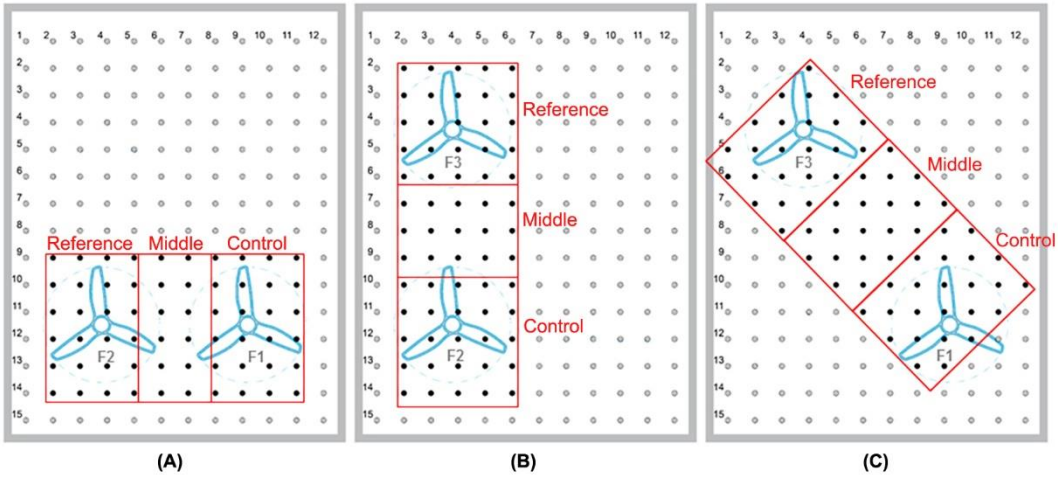

Figure A.1. Fan configurations in a double-fan room with different center-to-center distances: (A) 1.3x*D*; (B) 1.7x*D* and (C) 2.1x*D*.

Our approach is based on the concept of the control variable. By setting a constant speed level j (j = high, medium, low) to one fan (reference fan) while changing the speed of the other fan (control fan), speed level i (i = high, medium, low), we measured the corresponding air speed at measurement points within the covering area. As shown in Figure 5, increasing the speed of one fan will affect not only the air speed directly under the fan but also beneath the other fan and in the zone between them. However, the magnitudes of the interacted air speeds are different at these different areas. To avoid any computational misleading, we classified the covering area into three zones for each configuration as shown in Figure A.1: Reference zone (below reference fan), Middle zone, and Control zone (below control fan). We investigated the ratio of the air speed change caused by the combination of two fans to the air speed generated only by reference fan at each measurement point in the corresponding zone. The higher the absolute value of the ratio is, the stronger effect the control fan takes on the air speed change in each analyzed zone.

Within a certain zone in a certain fan configuration, the interactional speed ratio index (*ISR*) of control fan with speed i on reference fan with speed j is defined as

$$ISR_{i,j} = \frac{1}{n}\sum_{k=1}^{n}\frac{V_{C_i,R_j}(k)-V_{0,R_j}(k)}{V_{0,R_j}(k)} \quad \text{(A1)}$$

where $V_{C_i,R_j}(k)$ and $V_{0,R_j}(k)$ are the air speed at the k^{th} measuring point when speed settings of control and reference fans are (i, j) and (0, j) respectively. k = 1, 2, …, n and the value of n depends on the configuration and the zone as shown in Figure A.1. For example, if *ISR* in a certain zone is equal to

0.5, meaning that control fan causes a 50% overall increase of the air speed in that zone compared to the running of reference fan alone.

Table A.1 summarizes the *ISR* index values by combining different speed settings (high, medium and low) of the two fans for each zone and distance configuration. The air speed change in all zones depends on the relative speed levels of both fans. The impact of the control fan increases with the increase of the speed difference between fans (the increase of its speed level and the speed decrease of reference fan). In general, the increase of speed setting of the control fan affects mostly the Control zone (relative air speed change of 7-124%, 14-268% and 161-1817% for high, medium and low speed of reference fan respectively) and Middle zone subsequently (relative air speed change of 1-70%, 11-118% and 52-599% for high, medium and low speed of reference fan respectively). The lowest *ISR* values are observed in the Reference zone (relative air speed change of 5-13%, 0-17% and 1-199% for the high, medium and low speed of reference fan respectively).

Table A.1. Interactional speed ratio (*ISR*) index calculated based on (A1) by combining different fan speed settings for different configurations.

Control Ref.		H			M			L		
		Ref. zone	Middle zone	Control zone	Ref. zone	Middle zone	Control zone	Ref. zone	Middle zone	Control zone
		$(V_{C_H,R_H} - V_{0,R_H})/V_{0,R_H}$			$(V_{C_M,R_H} - V_{0,R_H})/V_{0,R_H}$			$(V_{C_L,R_H} - V_{0,R_H})/V_{0,R_H}$		
H	1.3x*D*	-0.07	0.43	0.93	-0.10	0.21	0.07	-0.10	-0.01	-0.28
	1.7x*D*	-0.07	0.70	1.24	0.09	0.46	0.42	0.13	-0.13	-0.21
	2.1x*D*	0.08	0.32	1.09	-0.05	0.13	0.66	-0.11	-0.28	-0.40
		$(V_{C_H,R_M} - V_{0,R_M})/V_{0,R_M}$			$(V_{C_M,R_M} - V_{0,R_M})/V_{0,R_M}$			$(V_{C_L,R_M} - V_{0,R_M})/V_{0,R_M}$		
M	1.3x*D*	-0.06	0.78	1.55	0.00	0.30	0.92	-0.17	-0.11	-0.25
	1.7x*D*	0.03	1.18	2.68	-0.08	0.73	1.32	0.07	0.28	0.14
	2.1x*D*	0.15	0.68	1.75	0.07	0.33	1.07	-0.09	-0.25	-0.37
		$(V_{C_H,R_L} - V_{0,R_L})/V_{0,R_L}$			$(V_{C_M,R_L} - V_{0,R_L})/V_{0,R_L}$			$(V_{C_L,R_L} - V_{0,R_L})/V_{0,R_L}$		
L	1.3x*D*	1.63	5.99	11.59	0.86	3.22	6.73	-0.01	0.69	1.61
	1.7x*D*	1.99	4.79	17.86	1.55	4.59	11.48	0.49	0.94	2.28
	2.1x*D*	0.99	4.16	18.17	0.36	2.59	12.35	0.10	0.52	2.76

Note that the proposed *ISR* index describes the relative effect of control fan on the air speed values, rather than the absolute interaction between the two fans. Consider Case 9 and 18 as an example, where speed levels of control and reference fans were high and medium respectively. Figures 8 and 9 indicate that space between fans is more affected by fan interaction at 1.3x*D* (Case 9) than at 1.7x*D* (Case 18) because the overall air speed is higher. However, *ISR* indexes for these two cases indicate that control fan has a more relative effect in the Middle zone at 1.7x*D* (*ISR* = 1.18) than at 1.3x*D* (*ISR* = 0.78). This is because both the denominator and numerator in Equation 1 are larger at 1.3x*D* (Case 9) than at 1.7x*D* (Case 18), and thus the quotient of them may not be larger. In summary, 1.3x*D*

(Case 9) has a stronger absolute interaction than 1.7x*D* (Case 18) in the Middle zone, but control fan at this distance has quantitively smaller relative effect than at 1.7x*D*. If we consider only one-configuration scenario (the distance between the fans is fixed), the proposed *ISR* index can also be used to quantify the absolute interaction between the fans.

To further interpret the data, especially to investigate the effect of the distance on the *ISR*, we plot the data according to different zones in Figure A.2. We considered three scenarios of the relative speed setting of the control fan compared to the reference fan: 1) lower speed (1st row), 2) the same speed (2nd row) and 3) higher speed (3rd row). In the first row, the control fan with low (L) speed hardly has any quantitative effect on the reference fan with medium or high speed. Only when the speed of the control fan increases to medium (M), we see a substantial increase of air speed in the Middle zone (we care more about Reference and Middle zones than Control zone). The maximum *ISR* (around 0.4) appears at the distance of 1.7x*D*. In the second row when the two fans are set with the same speed, we still do not see the significant quantitative effect in Reference zone. The relatively greater ratio value in L-L case (red) is limited by the trivial absolute magnitude of air speed itself. However, we can observe that the *ISR* index at distance of 1.7x*D* dominates in the Middle zone. An interesting observation is that the effect indexes for M-M and H-H cases at all three distances in all three zones are almost the same. The interaction between the two fans reaches a constant quantitative balance with the same relatively high speed settings (not for the case of L-L). This observation is consistent with the measurement results and smoke visualization. In the third row when the control fan can produce airflow with higher air speed than the reference fan, we finally observe the explicit quantitative effect (index can be over 1 for 1.7x*D*) in the Reference zone. In addition, the effect indexes at the distances of 1.3x*D* and 1.7x*D* are greater than 2.1x*D* in both the Reference and the Middle zones. The key observations are summarized as follows:

1. As mentioned above, the control zone is most affected (Figure A.2).
2. When the speed of control fan is lower than reference fan (1st row in Figure A.2), *ISR* is less than 0.5 and 1.7x*D* distance (red) has the most relative effect between the fans in Reference and Middle zones.
3. When both the fan are set with the same speed (2nd row in Figure A.2), *ISR* is less than 1 and 1.7x*D* distance (red) has the most relative effect in Reference and Middle zones. In Control zone, *ISR* is between 1 and 3, and this is a large relative effect in the zone.
4. When the speed of control fan is higher than reference fan (3rd row in Figure A.2), *ISR* can be higher than 1 for 1.7x*D* distance (red) in Reference zone, and can reach very high levels in Middle and Control zones.
5. In all scenarios (1st ~ 3rd row in Figure A.2C), 1.3x*D* distance (blue) has the least relative effect in Control zone.

DOI: 10.1016/j.buildenv.2018.06.037
https://escholarship.org/uc/item/2mk3n264

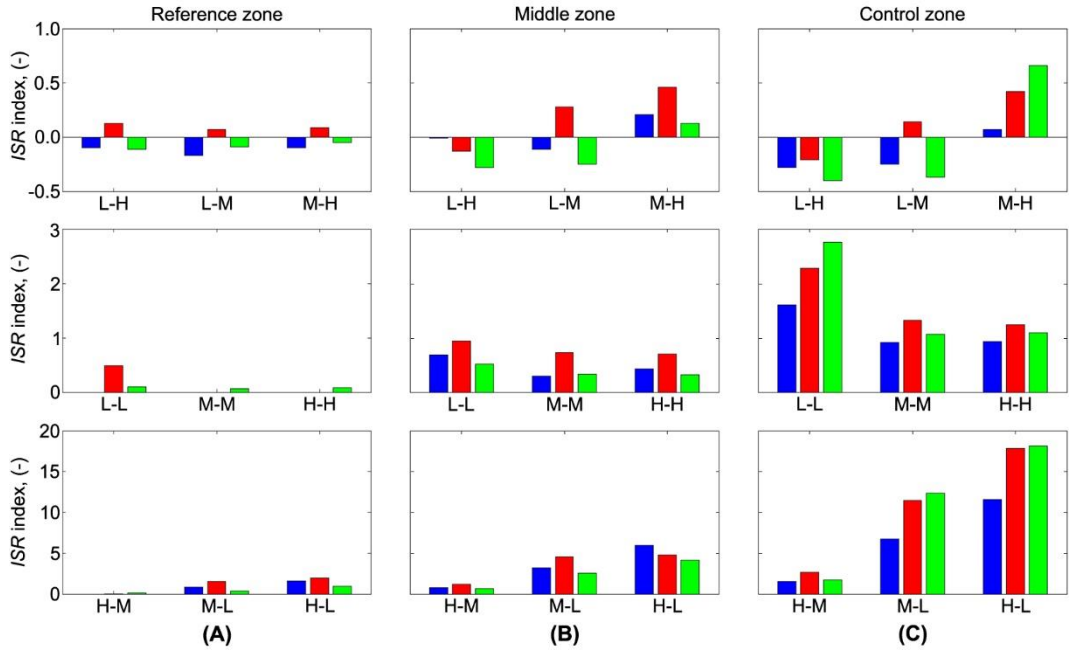

Figure A.2. Interactional speed ratio (*ISR*) at different center-to-center distance (blue: 1.3x*D*; red: 1.7x*D* and green: 2.1x*D*) and relative fan levels (Control – Reference fan) in different zones: (A) reference zone; (B) middle zone and (C) control zone. 1st row shows cases when Control fan was at speed level lower than Reference fan, 2nd row cases with fans at equal speed level and 3rd row with Control fan at speed level higher than Reference.

In this section, we studied the relative effect from a control fan on a reference fan quantitatively. Both the difference of fan speed levels and the distance between the fans play a key role in the interactive effect. Generally, the control fan has a more relative effect on the reference fan with increased speed. The interaction between the two fans can reach a balance when they are set to the same relatively high speed. It is not always the case that the closest distance between the fans has the most relative effect. The proposed effect index is an effective way to assess the interactive effect between fans quantitatively.

DOI: 10.1016/j.buildenv.2018.06.037
https://escholarship.org/uc/item/2mk3n264

Appendix B. User manual for the online visualization tool

To view the online air speed measurement for single-fan and double-fan cases, please go to the following links respectively, where average values are plotted:

single-fan case: https://cbe-berkeley.shinyapps.io/single-fan

double-fan case: https://cbe-berkeley.shinyapps.io/two-fans

The raw measurement data can be downloaded via the separate CSV files attached as Supplementary Information. The average air speeds are displayed as a 15×12 matrix (according to the measuring-point layout in Figure 1 in the paper) from a height of 1.7 m to 0.1 m, following the order from Speed 7 to 1, and Case 1 to 28, for single- and double-fan cases respectively.

The online visualization tool is based on Shiny-app–an R package combining abilities of R with the interactivity of the modern web. The user-friendly UI makes it easy for users to interact with our data and data analysis. The following sections provide a tutorial on how to use this tool.

Single-fan webpage

In the single-fan webpage, there are four blocks: 1) toolbar, 2) plane views in a specific height, 3) planes views in averaged heights, and 4) section views. The blocks are described in details as follows.

First row: the toolbar (upper block in Figure B.1). The toolbar provides the following functions:

1. Users can select fan speed level from 7 to 0. The default speed is Level 7. This function applies to all the remaining three blocks.
2. Users can select the row/column number for section views. The default choices are Row 8 and Column 7, which are the closest to the sections crossing the fan center.
3. Users can change the air speed scale range freely. The tool provides two modes: self-selected and min-max. In 'self-selected' mode, users can choose freely any sub-set of range from 0 to 3 m/s, while 'min-max' mode is based on the minimum and maximum of air speed under the specific speed level selected. This function applies to all the remaining three blocks.

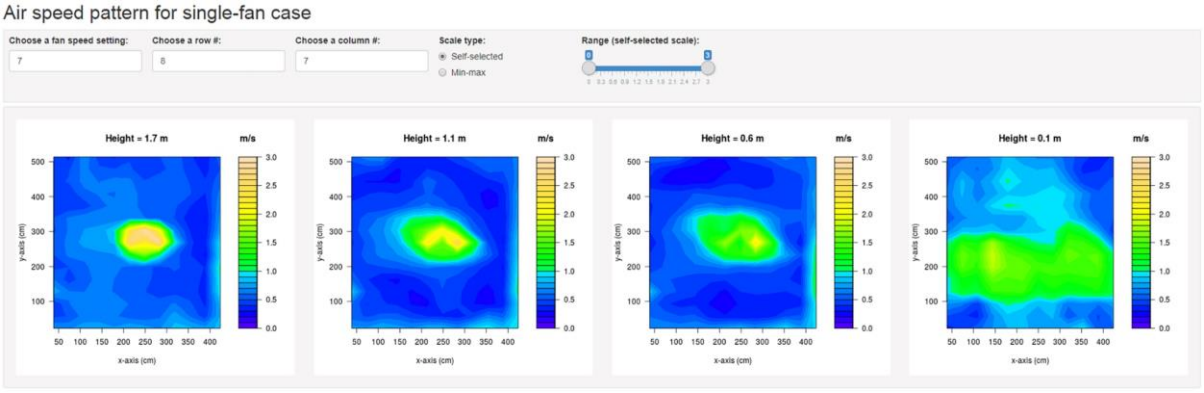

Figure B.1. Toolbar (upper block) and plane views in a specific height (lower block) in the single-fan webpage.

Second row: plane views in a specific height (lower block Figure B.1). This block consists of four sub-plots of air speed distributions in four horizontal planes, 1.7, 1.1, 0.6 and 0.1 m above the floor respectively. Users can change the range scale in the toolbar mentioned above.

Third row: plane views in averaged heights (Figure B.2). This block consists of three sub-plots. According to ASHRAE 55 [25], 0.1, 0.6 and 1.1 m are considered for the thermal comfort of a seated person, while 0.1, 0.6 and 1.7 m are for a standing person. The averaged four-height air speeds are also provided for easy reference. Users can change the range scale in the toolbar mentioned above.

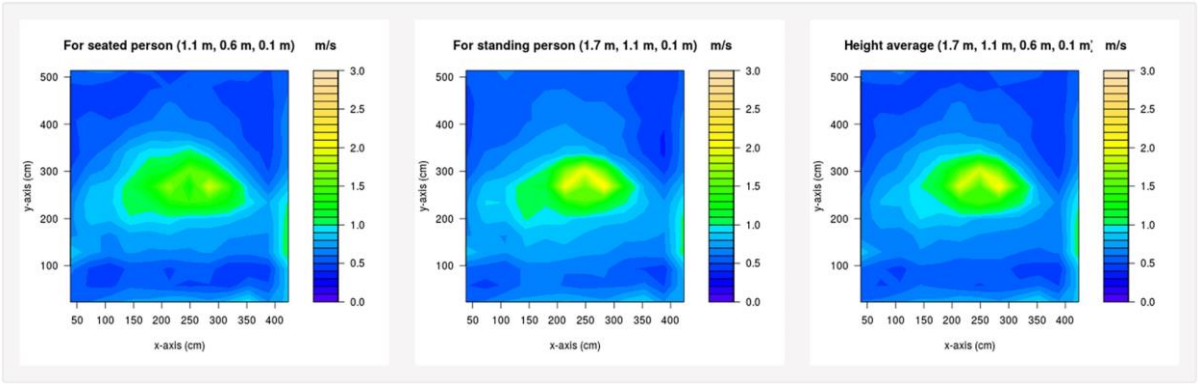

Figure B.2. Plane views in averaged heights in the single-fan webpage.

Fourth row: section views (Figure B.3). This block consists of two sub-plots of row- and column-wise vertical sections of air speed, respectively. To use this function, users should choose the specific row or column number from the toolbar, based on the measuring-points layout (as shown in Figure 1 in the paper). The default choices are the 8th row and 7th column, which are the closest to the sections crossing the fan center. Users can change the range scale in the toolbar mentioned above.

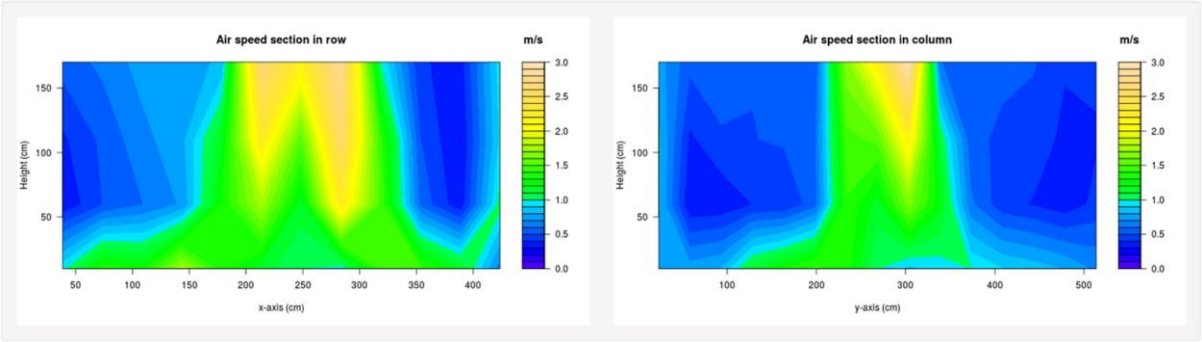

Figure B.3. Section views in a single-fan webpage.

Double-fan webpage

For the blocks in the double-fan webpage, the only difference from single-fan one is that there is an additional block of height-wise plane views for comparing two cases. The default choices are both Case 10. The blocks are described in details as follows.

First row: the toolbar (Figure B.4). The toolbar in double-fan webpage provides the function to choose two different cases in height-wise plane views for comparison. Besides, all the other functions are the same as the one in the single-fan webpage.

Figure B.4. Toolbar in the double-fan webpage.

DOI: 10.1016/j.buildenv.2018.06.037
https://escholarship.org/uc/item/2mk3n264

Second row: height-wise plane views in 1st case. This block provides the plane views in four heights based on the 1st case choice of users'. Users can change the range scale in the toolbar.

Third row: height-wise plane views in 2nd case. This block provides the plane views in four heights based on the 2nd case choice of users'. Users can change the range scale in the toolbar.

Fourth row: plane views in averaged heights. This block provides the averaged-heights plane views based on users' 1st case choice, the same as the ones in the single-fan webpage. Users can change the range scale in the toolbar.

Fifth row: section view. This block provides the section views based on users' 1st case choice, the same as the ones in the single-fan webpage. The default choices are the 11th row and 7th column. Users can change the range scale in the toolbar.

DOI: 10.1016/j.buildenv.2018.06.037
https://escholarship.org/uc/item/2mk3n264

Appendix C. Calculation methodology based on the ASHRAE 216P

Weighting factor (*WF*). Weighting factors are a ratio of the area represented by a test position to the total area. They are calculated for each test positions (*n* = 0, ..., max) according to following equations:

$$WF_0 = \frac{\left(\frac{d_{n=1}}{2}\right)^2}{(d_{max})^2} \quad \text{(C1)}$$

$$WF_n = \frac{\left(\frac{d_n + d_{n+1}}{2}\right)^2 - \left(\frac{d_n + d_{n-1}}{2}\right)^2}{(d_{max})^2} \quad \text{(C2)}$$

$$WF_{max} = \frac{(d_{max})^2 - \left(\frac{d_{max} + d_{max-1}}{2}\right)^2}{(d_{msx})^2} \quad \text{(C3)}$$

where: d_n – radial distance from the *n* test position to the fan center.

Room average air speed. Room average air speed should be calculated separately for the standing and seating posture based on the mean values at each test position (*n* = 0, …, max):

$$v_{a,m,seated,room} = \sum_{n=0}^{max} WF_n \times v_{a,m,seated,n} \quad \text{(C4)}$$

$$v_{a,m,standing,room} = \sum_{n=0}^{max} WF_n \times v_{a,m,standing,n} \quad \text{(C5)}$$

where:

$v_{a,m,seated,n}$ – seated average air speed value, calculated from mean values recorded at 0.1, 0.6 and 1.1 m at the *n* test position,

$v_{a,m,standing,n}$ – standing average air speed value, calculated from mean values recorded at 0.1, 1.1 and 1.7 m at the *n* test position.

Room average cooling effect (*CE*). The cooling effect calculated as a difference in SET* [25] between baseline values (v_a = 0.1 m/s) and room average air speed. Remaining values of comfort parameters are assumed: $t_a = t_{mr}$ = 26.8 °C, x = 0.010 kg/kg, M = 1.1 met, I_{cl} = 0.5 clo. The room average cooling effect should be calculated separately for seated and standing occupancy according to follow equations (for SI units):

$$CE_{a,m,seated,room} = \sum_{n=0}^{max} WF_n \times 1.53 \times \ln\left(v_{a,m,seated,n}\right) + 3.444 \quad \text{(C6)}$$

$$CE_{a,m,standing,room} = \sum_{n=0}^{max} WF_n \times 1.53 \times \ln\left(v_{a,m,standing,n}\right) + 3.444 \quad \text{(C7)}$$

Cooling coverage fraction (*CC*). It is a fraction of the room area where average air speed is higher or equal to 0.43 m/s (for which *CE* = 2.2 °C). It is defined separately for seated and standing position:

$$CC_{seated} = \sum_{n=0}^{max} WF_n \times Y_{n,seated} \quad \text{(C8)}$$

$$CC_{standing} = \sum_{n=0}^{max} WF_n \times Y_{n,standing} \quad \text{(C9)}$$

where:

Y_n = 1 if seated/standing average air speed at *n* test position is greater or equal to 0.43 m/s,

Y_n = 0 if seated/standing average air speed at *n* test position is lower 0.43 m/s.